

Thunderbolt: Concurrent Smart Contract Execution with Nonblocking Reconfiguration for Sharded DAGs

Junchao Chen, Alberto Sonnino^{§‡}, Lefteris Kokoris-Kogias[‡], Mohammad Sadoghi

Exploratory Systems Lab

University of California, Davis

[‡] MysterLabs

[§] University College London (UCL)

Abstract

Sharding has emerged as a critical technique for enhancing blockchain system scalability. However, existing sharding approaches face unique challenges when applied to Directed Acyclic Graph (DAG)-based protocols that integrate expressive smart contract processing. Current solutions predominantly rely on coordination mechanisms like two-phase commit (2PC) and require transaction read/write sets to optimize parallel execution. These requirements introduce two fundamental limitations: (1) additional coordination phases incur latency overhead, and (2) pre-declaration of read/write sets proves impractical for Turing-complete smart contracts with dynamic access patterns.

This paper presents Thunderbolt, a novel sharding architecture for both single-shard transactions (Single-shard TXs) and cross-shard transactions (Cross-shard TXs) and enables nonblocking reconfiguration to ensure system liveness. Our design introduces four key innovations: First, each replica serves dual roles as a full-shard representative and transaction proposer (shard submitter), employing differentiated execution models: the Execution-Order-Validation (EOV) model for Single-shard TXs and Order-Execution (OE) model for Cross-shard TXs. Second, we develop a DAG-based coordination protocol that establishes deterministic ordering between two transaction types while preserving concurrent execution capabilities. Third, we implement a dynamic concurrency controller that schedules Single-shard TXs without requiring prior knowledge of read/write sets, enabling runtime dependency resolution. Fourth, Thunderbolt introduces a nonblocking shard reconfiguration mechanism to address censorship attacks by featuring frequent shard re-assignment without impeding the construction of DAG nor blocking consensus. This approach maintains continuous DAG construction and consensus progress while preventing persistent adversarial control through periodic shard reassignment. Thunderbolt achieves a 50x throughput improvement with 64 replicas compared to serial execution in the Tusk framework.

ACM Reference Format:

Junchao Chen, Alberto Sonnino^{§‡}, Lefteris Kokoris-Kogias[‡], Mohammad Sadoghi. 2025. Thunderbolt: Concurrent Smart Contract Execution with

Permission to make digital or hard copies of all or part of this work for personal or classroom use is granted without fee provided that copies are not made or distributed for profit or commercial advantage and that copies bear this notice and the full citation on the first page. Copyrights for components of this work owned by others than the author(s) must be honored. Abstracting with credit is permitted. To copy otherwise, or republish, to post on servers or to redistribute to lists, requires prior specific permission and/or a fee. Request permissions from permissions@acm.org.

Conference'17, July 2017, Washington, DC, USA

© 2025 Copyright held by the owner/author(s). Publication rights licensed to ACM.

ACM ISBN 978-x-xxxx-xxxx-x/YY/MM

<https://doi.org/10.1145/nnnnnnnn.nnnnnnnn>

Nonblocking Reconfiguration for Sharded DAGs. In . ACM, New York, NY, USA, 18 pages. <https://doi.org/10.1145/nnnnnnnn.nnnnnnnn>

1 Introduction

The emergence of blockchain technology has spurred significant interest in developing resilient systems capable of processing data and transactions under Byzantine conditions, including software errors, hardware failures, network disruptions, and coordinated malicious attacks [7, 10, 28, 34, 41, 62]. These systems enhance reliability and security by enabling collaboration among multiple independent participants [18, 31, 43, 46, 60, 61, 63, 66, 94].

Smart contracts [85, 86], as programmable transaction frameworks embedded in blockchain platforms, empower developers to address real-world challenges through decentralized solutions [17, 52]. However, their adoption is often hindered by execution delays caused by runtime contract code analysis [5]. To overcome this limitation, researchers are actively exploring performance optimization strategies for contract-based blockchain systems.

Several strategies have emerged to improve execution within blockchain systems.

Transaction Processing Models: One practical approach involves enhancing transaction processing. Most blockchain systems adopt the Order-Execute (OE) model, where transactions are ordered through consensus before execution [19, 36, 38, 99]. OE-based systems often employ deterministic concurrency controls by constructing transaction dependency graphs to optimize parallelism [29, 67, 93, 98]. In contrast, platforms like Hyperledger Fabric [10] utilize the Execute-Order-Validate (EOV) model, executing transactions before consensus to enhance flexibility and enable concurrency protocols such as Optimistic Concurrency Control (OCC) [51].

Scalability via DAG and Sharding: Another critical area for advancement in blockchain technology is scalability, particularly in supporting parallel execution. Recent advancements leverage Directed Acyclic Graph (DAG)-based consensus protocols to improve scalability. These protocols enable replicas to submit proposals concurrently by building a DAG that links new proposals to historical ones. This architecture has gained significant recognition in the industry due to its robust security features, exceptional scalability, and capability to support smart contracts [11, 12, 23, 48, 49, 57, 71, 79, 82–84]. Complementary to DAG-based approaches, sharding techniques allow parallel transaction processing across independent shards, reducing consensus overhead [4, 24, 39, 42, 50, 81, 97, 104, 105, 107].

However, the above approaches do not effectively improve the execution of smart contracts:

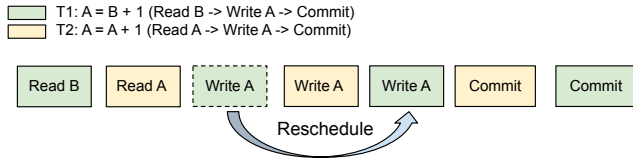


Figure 1: A transaction reschedule to avoid abortion by moving the *WriteA* on T_1 after the *WriteA* on T_2 . They all obtain the correct result based on their operations without any conflict.

Challenge1: Enhancing Transaction Parallelism without advanced knowledge. While *OE*-based solutions leverage dependency graphs to optimize parallelism, they require prior knowledge of transaction read/write sets, a constraint incompatible with dynamic smart contracts. Conversely, *EOV*-based approaches face high transaction conflict rates, necessitating advanced conflict resolution algorithms.

Challenge2: Efficient Cross-Shard Transaction Processing. Existing solutions for cross-shard atomicity, such as relay-based protocols (Sharper [8], BrokerChain [45], and SharDAG [21]) and traditional Two-Phase Commit (2PC) [24, 44], introduce significant delays due to inter-shard coordination. While multi-shard consensus [8, 68] mitigates 2PC limitations, it sacrifices scalability in large-scale networks with high contention.

The challenges described above raise the question of whether it is possible to design a sharding system that does not depend on understanding the read and write sets of transactions, nor requires additional coordinators to manage cross-shard transactions.

We propose Thunderbolt, an innovative sharding architecture that seamlessly processes both single-shard (Single-shard TXs) and cross-shard transactions (Cross-shard TXs) without centralized coordinators. Thunderbolt effectively integrates the *OE* and *EOV* models, where the *EOV* model enhances parallelism in the execution of Single-shard TXs, while the *OE* model minimizes the abort rate when handling Cross-shard TXs across different shards. Furthermore, the *OE* model ensures a coordinated execution order between these two types of transactions, maintaining the overall correctness of the execution process.

Similar to conventional sharding systems, Thunderbolt organizes transactions into distinct shards to mitigate potential conflicts. In particular, each replica within Thunderbolt corresponds to a single shard and acts as a shard submitter, proposing transactions within that shard. Thunderbolt employs a DAG-based consensus protocol [11, 12, 23, 48, 49, 57, 79, 82–84] to reach an agreement on the execution results provided by each shard submitter.

Inspired by Sui's epoch switching [15], Thunderbolt employs round-robin scheduling [72] to rotate shard submitters periodically, enhancing the system's security and liveness. Submitter rotation is triggered on-demand if a shard fails to propose transactions within a timeout, with seamless DAG transitions preserving protocol continuity.

Thunderbolt also introduces a concurrent executor (*CE*) designed to improve the execution of Single-shard TXs before reaching consensus. Unlike traditional concurrency protocols that primarily manage conflicts based on the order of arrival [3, 30, 87], the *CE*

utilizes a nondeterministic ordering system based on the execution run-time states of each transaction. This innovative approach minimizes the abort rate, thereby reducing transaction latency. As illustrated in Figure 1, the *CE* effectively reschedules transactions based on their run-time executions to prevent aborts. For instance, transaction T_2 , which would ordinarily conflict with the write operation of transaction T_1 , can be successfully committed without cancellation.

In summary, this paper makes the following contributions.

- To our knowledge, Thunderbolt is the first sharding consensus mechanism that combines the *OE* and *EOV* models based on DAG-based protocols without requiring any additional coordinators to determine the order between Single-shard TXs and Cross-shard TXs.
- We introduce a new concurrency paradigm that implements a parallel preplay for Single-shard TXs (concurrent consensus execution). Thunderbolt preplays Single-shard TXs followed by parallel verification without needing prior knowledge of the read/write sets.
- Thunderbolt features a nonblocking shard reconfiguration protocol that allows for the rotation of shard assignments without pausing either DAG dissemination or the consensus layer.
- We have implemented a concurrent executor to enhance the parallelism of executing smart contracts without prior knowledge of the read/write sets on Single-shard TXs. The execution engine dynamically arranges transactions based on current assessments to reduce abort rates due to conflicts.
- Our evaluation of Thunderbolt demonstrates an impressive 50x speedup over Tusk [23] with sequential execution using the SmallBank workload on 64 replicas built on Apache ResilientDB (Incubating) [2, 38].

2 Background

2.1 Smart Contract

A smart contract is a digital protocol, introduced by Nick Szabo in the mid-1990s [85], designed to facilitate, verify, or enforce the negotiation or performance of a contract automatically. Unlike traditional contracts, which rely on legal systems for enforcement, smart contracts are self-executing and operate on blockchain technology. They are written in code and run on decentralized platforms like Ethereum, ensuring transparency, security, and immutability. Smart contracts eliminate the need for intermediaries, reduce the risk of fraud, and enable trustless transactions between parties. They are widely used in various applications, including decentralized finance (DeFi), supply chain management, and digital identity verification.

These contracts consist of custom functions that operate on user accounts with associated balances. Once deployed to the network, transactions invoking the functions specified in the contract are proposed to execute predefined operations that interact with the user accounts. However, the execution of the contract code occurs within the Ethereum Virtual Machine (EVM) [58], which results in the read and write sets of the contract being indeterminate prior to execution.

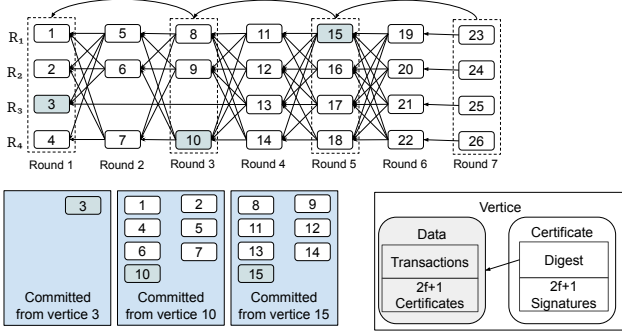


Figure 2: Overview of a DAG-based protocol on Tusk generated by 4 replicas. Each vertex contains both data and a certificate. Each data refers to $2f + 1$ certificates from the previous round. Each certificate is generated from its corresponding data, which has received signatures from $2f + 1$ replicas. The leader vertex for round r , the solid vertex used to commit the data in its causal history, will be determined before processing round $r + 2$.

2.2 DAG-based protocols

Thunderbolt leverages a Directed Acyclic Graph (DAG) structure to address scalability challenges in blockchain systems. This architecture enables efficient transaction proposal mechanisms while maintaining robust security, high throughput, and native support for smart contracts. DAG-based protocols have gained significant traction in the industry due to their ability to decouple transaction dissemination from consensus processes [11, 12, 23, 48, 49, 57, 71, 79, 82–84].

In contrast to traditional linear blockchains, DAG-based protocols allow multiple replicas to propose transactions concurrently. These transactions are constructed into a deterministic DAG structure, ensuring a consistent topological ordering across all honest replicas. Recent advancements in this domain, including Tusk [23, 83], BBCA-Chain [57], Shoal/Shoal++ [11, 82], Mysticeti [13], and Cordial Miners [49], demonstrate how DAGs streamline consensus by separating data propagation from finality mechanisms.

The protocol operates in synchronized rounds, where each DAG vertex in a round consists of two components:

- Data Payload: Contains transactions and references to at least $2f + 1$ certificates from the prior round.
- Certificate: A quorum of $2f + 1$ cryptographic signatures attesting to the validity of the vertex and its dependencies.

During each round, replicas broadcast their proposed vertices to the network. A vertex becomes certified once $2f + 1$ signatures are collected, enabling it to serve as a dependency for new vertices in subsequent rounds. This iterative process ensures liveness while preserving the DAG's causal ordering.

Vertex finalization occurs at fixed intervals, typically every two rounds in Tusk [23] or three rounds in DAG-Rider [48]. A designated leader (selected via round-robin scheduling [72] or distributed randomness [16]) proposes a vertex for commitment. A leader vertex in round r is eligible to be committed during round $r + 2$ (as in Tusk): 1) The replica must have received at least $2f + 1$ vertices

from round $r + 1$, and 2) The leader vertex must be referenced by a minimum of $f + 1$ vertices in round $r + 1$.

DAG-based protocols provide the following properties:

- Validity: if an honest replica R has a vertex B in its local view of the DAG, then R also has all the causal history of B .
- Consistency: if an honest replica R obtains a vertex B_r in round r from replica P , then, eventually, all other honest replicas will have B_r .
- Completeness: if two honest replicas have a vertex B_r in round r , then the causal histories of B_r are identical in both replicas.

3 Thunderbolt Overview

Thunderbolt advances smart contract execution efficiency through an innovative sharding architecture augmented by a dynamic shard reconfiguration mechanism. This mechanism counters potential censorship attacks, such as post-execution transaction suppression or biased transaction selection, ensuring network integrity.

Unlike conventional sharding systems that partition replicas into isolated groups governed by separate consensus protocols, Thunderbolt employs a single unified consensus protocol jointly maintained by all replicas. Each replica operates as a shard submitter, processing transactions specific to its assigned shard. To coordinate cross-shard transaction ordering and execution, Thunderbolt leverages a DAG-based consensus protocol, enabling global agreement on transaction validity while preserving shard-level parallelism. For the sake of clarity in the accompanying illustrations, the terms "replicas" and "shard submitters" may be used interchangeably.

Thunderbolt employs both *EOV* model and *OE* model to address Single-shard TXs and Cross-shard TXs.

- Single-shard TXs (*EOV* Model): Transactions confined to a single shard are processed non-deterministically by a Concurrent Executor (CE) within the corresponding shard submitter. After the local preplay, results undergo a consensus across all shards to ensure state consistency.
- Cross-shard TXs (*OE* Model): Cross-shard TXs employ an optimistic concurrency control protocol with deterministic finalization. Atomic commitment is achieved post-consensus, allowing tentative execution optimistically while guaranteeing rollback-free confirmation.

Figure 3 demonstrates an example where two shard submitters propose two single-shard transactions. Further details on Single-shard TXs and Cross-shard TXs are provided in Section 4 and Section 5.

Thunderbolt also allows the migration of each shard to another replica to avoid a censorship attack, such as dropping transactions.

3.1 System and Data Model

In this section, we describe the system and the data model. We leave the discussion of the Single-shard TXs in Section 4, the Cross-shard TXs in Section 5, and the shard reconfiguration in Section 6.

System model. We assume a set of n replicas, of which at most f are faulty, $n = 3f + 1$. The f faulty replicas can perform any arbitrary (Byzantine) failures, while the remaining replicas are assumed to be honest and follow the protocol's specifications at all times. We

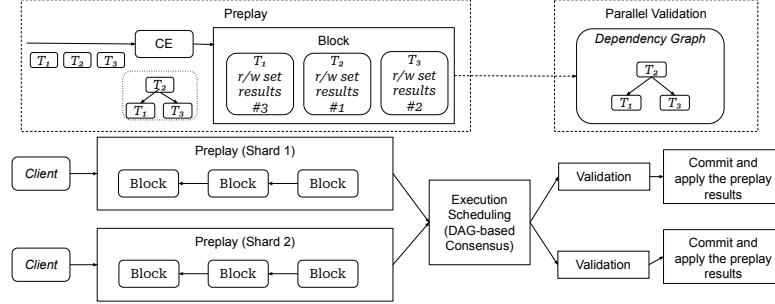


Figure 3: Single-shard TXs in each shard will be preplayed by the *CE* to obtain their preplay outcomes. Subsequently, the blocks containing these preplay outcomes will achieve a global order through a DAG-based consensus protocol, which each replica will then validate. The validation process will generate a dependency graph based on the read/write sets included within the blocks, enhancing parallelism in the system.

assume an eventually synchronous network [27] that messages sent from a replica will ultimately arrive in a global stabilization time (*GST*), which is unknown to the replicas. We also assume communications between replicas go through authenticated point-to-point channels, and messages are authenticated by a public-private key pair signed by the sender.

Data model. The data model assumes that each transaction includes a contract code with functions to access data belonging to the sender in the shard. The contract involves two types of operations: $\langle \text{Read}, K \rangle$ and $\langle \text{Write}, K, V \rangle$. Here, K represents the key required for access and V is the value that needs to be written to the key K . The contract code is Turing-complete and users could not obtain any information without execution. We also assume that the functions of the contract are idempotent.

Thunderbolt partitions users and their data into distinct shards. To ensure data is distributed across shards, users must assign a shard ID (*SID*) to each key, specifying the shard where the key resides. These (*SIDs*) serve a dual purpose: they direct transactions to the corresponding shard submitter and enable parallel processing across multiple shards, enhancing system efficiency (Section 5.1).

4 Single Shard Transactions

Thunderbolt processes Single-shard TXs through three core components: preplay, execution scheduling, and validation. During each round, a shard submitter initiates the workflow by preplaying a batch of Single-shard TXs. This generates a block containing critical preplay outcomes, which the submitter propagates to other shards via a DAG-based consensus protocol. During consensus, these blocks undergo parallel validation across shards. Once a replica commits a block, it applies the preplay results to its storage.

4.1 Preplay

In Thunderbolt, shard submitters play a pivotal role by preplaying transactions to determine their outcomes before block creation. A concurrent executor (*CE*) is employed to preprocess batches of transactions efficiently, producing detailed outputs for each transaction. These outputs include: the read/write sets accessed during execution, the corresponding execution results, and a scheduled execution order (as depicted in Figure 3).

The scheduled order establishes a deterministic serialized sequence, ensuring transaction results remain consistent when executed in the prescribed order. The read/write sets reveal the specific data accessed by each transaction. Crucially, these sets cannot be predetermined and are derived exclusively through the preplay process.

4.2 Execution Scheduling

Thunderbolt integrates with any DAG-based dissemination layer that employs a consensus protocol to establish a total block order across replicas. In each round r , a shard submitter R proposes a *CE*-generated block to the DAG, creating a new vertex in the graph. This vertex links to all prior vertices, including those proposed by R in round $r - 1$. For clarity, "vertices" in the DAG are hereafter referred to as "blocks" in the following sections, implying they have been certified by the protocol.

4.3 Validation

When a replica receives data for round r via the DAG (Section 2.2), Thunderbolt initiates a rigorous validation process to verify the integrity of preplay results within the blocks. Validators construct a local dependency graph using the read/write sets to enable parallel transaction validation rather than sequential checks, optimizing system throughput. Notably, blocks from round $r - 1$ are validated before those from round r for the same shard submitter.

During re-execution, validators confirm that the computed read sets match the values recorded in the block. A valid dependency graph guarantees consistent read-set results and ensures the final state of each key aligns with the block's declared values. If discrepancies in read-set values are detected, the block is flagged as invalid and discarded. Until blocks are committed, replicas retain preplay results in local storage, either to process Cross-shard TXs (Section 5) or until DAG reconfiguration occurs (Section 6).

5 Cross-shard transactions

5.1 Rules for Proposals

Cross-shard TXs involve multiple shards and require exclusive execution to prevent conflicts with other transactions. Thunderbolt must, therefore, coordinate both the sequencing of Cross-shard

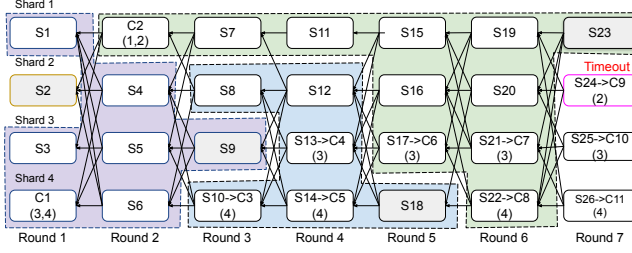


Figure 4: An example illustrates the commitment of each leader in the process of converting Single-shard TXs to Cross-shard TXs on Tusk. In this DAG, S_i denotes a Single-shard TX, while $C_i(\{X\})$ represents a Cross-shard TX associated with shards $\{X\}$. The leaders in the odd rounds are selected using round-robin selection. The blocks committed by the same leader have borders of the same color. S_i will be converted to C_i if there is any conflict blocks (S_{10}) or could not receive the leader block in time (S_{24}).

TXs within individual shards and their interactions with Single-shard TXs. Prior approaches often rely on coordinators to establish inter-shard order [8, 21, 24, 44, 45, 50, 68, 104], but these introduce communication overhead that degrades performance.

To address this, Thunderbolt leverages the DAG's predetermined leaders to enforce deterministic cross-shard execution. Since Single-shard TXs are preplayed (Section 4.1), Thunderbolt enforces a consistent partial order between single-shard and cross-shard transactions via the following rules:

- G1) If a leader L commits both a Single-shard TX and a Cross-shard TX, the Single-shard TX must be committed first.
- G2) If leader L_i commits Cross-shard TX X in round i , any Single-shard TX Y committed by leader L_j in round j (where $j > i$) cannot execute until X is finalized.

It is worth knowing that Leaders are predetermined per round using deterministic methods (e.g., round-robin or global random coins). To enforce these rules, Thunderbolt applies the following proposal rules:

- P1) Cross-shard TXs are submitted directly to the DAG, bypassing the CE .
- P2) Leaders committing a batch of transactions must finalize all Single-shard TXs before Cross-shard TXs.
- P3) If a shard submitter SL proposes a Single-shard TX X in round r , and the current round's leader L differs from SL , SL must:
 - Wait for L 's proposal before preplaying X .
 - Convert X to a Cross-shard TX if any uncommitted Cross-shard TX Y in L 's history conflicts with X .
 - Otherwise, preplay X and submit the results.
- P4) If a shard submitter SL proposes a Single-shard TX X in round r , and a prior leader's uncommitted Cross-shard TX Y (in round $q < r$) conflicts with X , SL converts X to a Cross-shard TX.
- P5) If leader L in round r commits a Cross-shard TX X related to shard A but lacks A 's proposal in round $r - 1$, L defers committing A and A 's subsequent proposals.

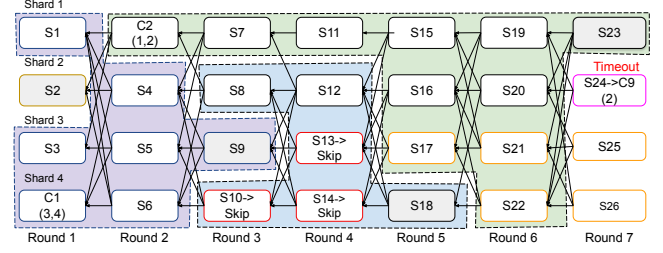


Figure 5: An example of proposing skipping blocks to restart the preplay of the Single-shard TXs. The Single-shard TXs (S_{17}, S_{21} , and S_{22}), which would be converted to Cross-shard TXs after round 5 in Figure 4, can replay their executions before delivering to the DAG.

- P6) If a shard submitter SL proposes a Single-shard TX X in round r but the leader L 's proposal is delayed beyond a timeout, SL converts X to a Cross-shard TX.

These rules enable Thunderbolt to process Cross-shard TXs without blocking shards while maximizing parallelism for single-shard transaction preplay.

EXAMPLE 1. Figure 4 illustrates Thunderbolt's handling of single-shard and cross-shard transactions on Tusk:

- Single-shard TXs will be executed before Cross-shard TXs under the same leader (Rule P2).
- S_{10} is converted to Cross-shard TX C_1 due to its dependency on S_9 's leader history (Rule P3).
- S_{13} and S_{14} become C_4 and C_5 , respectively, because C_1 remains uncommitted until round 5 (Rule P4).
- Leader S_{18} in round 5 skips C_2 and subsequent transactions due to missing S_{11} (Rule P5).
- In round 7, S_{24} converts S_4 to Cross-shard TX C_9 after failing to receive leader S_{23} 's proposal (Rule P6).

Detailed discussions of Rule P5 and Rule P6 follow in subsequent sections.

5.2 Parallel Execution

When processing Cross-shard TXs, Thunderbolt preserves all sharding metadata for each transaction. Rather than sequential execution, Thunderbolt employs deterministic concurrency control mechanisms, such as QueCC [67], to construct dependency graphs using cross-shard metadata (SID). This enables parallel execution while maintaining consistency across shards.

5.3 Message Failures

In practical deployments, network unreliability may delay message delivery. To mitigate this:

- If a leader L cannot include all Single-shard TXs linked to a Cross-shard TXs due to network delays (e.g., missing shard proposals), L bypasses the affected Cross-shard TX and subsequent transactions from the same shard (C_2 in Figure 4 on Rule P5). This prevents violations of global ordering G2 by excluding incomplete transaction sets. These transactions are later finalized by subsequent leaders.

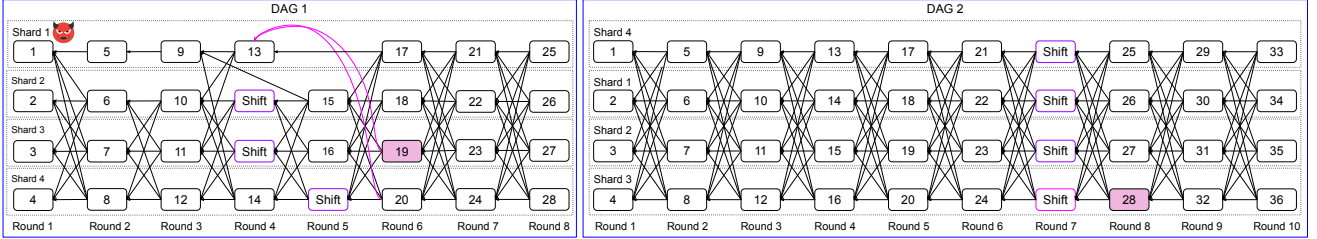


Figure 6: An example of DAG reconfiguration. Shard 1 in DAG 1 which is a malicious replica that delays the blocks from round 2, which triggers a reconfiguration to a new DAG ($K = 2$). Additionally, a further reconfiguration to DAG 2 will take place after the replicas have proposed six rounds ($K' = 6$).

- If a shard submitter fails to receive the leader's proposal within a round's timeout window, it cannot preplay its Single-shard TX (Rule P6). The submitter instead promotes the transaction to a Cross-shard TX and submits it directly to the DAG (such as S24 in Figure 4).

5.4 Preplay Recovering

Under Rule P3, a shard submitter SL must convert a Single-shard TX to a Cross-shard TX if it detects conflicting uncommitted Cross-shard TXs in prior leader histories. While this ensures safety, it forfeits the performance benefits of preplay, such as the blocks in shard 3 after round 3 in Figure 4.

To recover preplay, SL must verify that all conflicting Cross-shard TXs have been finalized by preceding leaders. Since a leader CL_r in round r is finalized within two subsequent rounds (Section 2.2), SL can safely preplay new single-shard transactions once: 1) It receives $2f + 1$ certificates in round $r + 1$, and 2) CL_r is referenced by at least $f + 1$ blocks in round $r + 1$. If SL identifies any conflicting Cross-shard TXs while proposing Single-shard TXs, SL submits skip blocks to the DAG until prior leaders are finalized. For instance, S10, S13, and S14 in Figure 5 are converted to skip blocks. Consequently, subsequent transactions, like S17 and S22, are reverted to the EOV model, restoring preplay capabilities.

6 Shards Reconfiguration

In Byzantine environments, compromised replicas may enable malicious actors to launch censorship attacks, threatening the integrity of transactions within their assigned shards.

Thunderbolt employs a round-robin selection mechanism [78] to rotate shard submitters if a leader fails to propose transactions for K rounds or at fixed intervals of K' rounds (where $K' > K$).

This rotation serves dual purposes:

- Preventing transaction duplication (DDOS [26, 59]): Submitters perform local deduplication to block malicious clients from flooding the system with redundant transactions, a known challenge in DAG-based protocols [12, 15, 83].
- Mitigating censorship: Regular rotation limits the window for a compromised submitter to disrupt operations.

Unlike traditional consensus protocols that depend on notification messages to alter primary nodes, Thunderbolt introduces an innovative mechanism that uses the underlying DAG protocols to facilitate the seamless transition to a new DAG and reconfigure shard submitters. We leverage a round-robin approach to select a

new submitter that if the current submitter of shard X is replica R_i , the subsequent submitter of shard X will be $R_{(i \bmod n)+1}$.

However, the transmission of blocks to a new submitter may experience delays or omissions due to network issues or the actions of a malicious submitter. If the new submitter for round r is unable to receive the proposal committed in round $r - 1$ from the previous submitter, the new submitter will stop operations until the block arrives to ensure safety.

To address this challenge, Thunderbolt introduces Shift blocks to reach agreements among shards when a shard reconfiguration should be initiated and switch to a new DAG to process further transactions.

A replica R in a shard broadcasts a Shift block in round r under the following conditions:

- (1) R receives no block from a shard submitter after round $r - K$.
- (2) R has proposed blocks for at least K' rounds.
- (3) R received $f + 1$ Shift blocks from distinct replicas at round $r - 1$.
- (4) R does not broadcast the Shift block before.

EXAMPLE 2. In Figure 6 where $K = 2$ and $K' = 6$, shards 2 and 3 broadcast Shift blocks in round 4 after failing to receive blocks from shard 1 in rounds 2–3. Despite receiving a block in round 4, shard 4 broadcasts a Shift block in round 5 upon receiving two Shift blocks from peers, prioritizing liveness assurance.

Non-blocking Reconfiguration. Since all honest replicas will commit the same block during the same round (Section 2.2), we designate the round of the first commit block that includes $2f + 1$ Shift blocks as the ending round for the current DAG. Then, **each replica will begin a new DAG from the same ending round to ensure the system's safety**. For instance, shard 2 will propose block 15 at round 5 after proposing a Shift block at round 4. Finally, block 19 from shard 3 at round 6 is selected as the leader during the consensus process. Subsequently, shard 3 commits all historical blocks from block 19, including the Shift blocks from other shards. At this point, all shards will transition to the new DAG (DAG 2) and start executing transactions within the new shard. Moreover, each replica will propose a Shift block every $K' = 6$ blocks in the new DAG (DAG 2) to facilitate a transition to the next DAG. This measure is intended to protect against censorship attacks, which may involve dropping transactions, failing to propose blocks, or prioritizing certain transactions over others.

Uncommitted Transactions. Due to the two-round leader commitment latency, transactions uncommitted in the ending round of

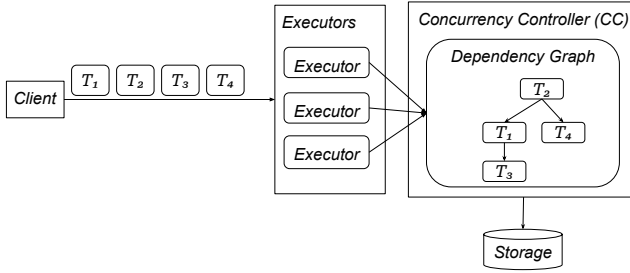


Figure 7: The architecture of the *CE* consists of a set of executors that execute transactions. The concurrency controller utilizes a dependency graph to determine the order of transactions and their execution results.

Time	Transactions	Operations	Dependencies	Execution Order
0	Initial DB	$D = 3$	\emptyset	\emptyset
1	$T_1:(W, D, 3)$	T_1 writes $D = 3$	$\{T_1\}$	\emptyset
2	$T_2:(R, D, 3)$	T_2 reads D on T_1 : ($D = 3$)	$\{T_1 \rightarrow T_2\}$	\emptyset
3	$T_3:(R, D, 3)$	T_3 reads D on T_1 : ($D = 3$)	$\{T_1 \rightarrow T_2, T_1 \rightarrow T_3\}$	\emptyset
4	T_3 : Commit	Wait for T_1	$\{T_1 \rightarrow T_2, T_1 \rightarrow T_3\}$	\emptyset
5	$T_1:(W, D, 5)$	T_1 writes $D = 5$. Abort T_2, T_3	$\{T_1\}$	\emptyset
6	$T_3:(R, D, 5)$ (Re-execute)	T_3 reads D on T_1 : ($D = 5$)	$\{T_1 \rightarrow T_3\}$	\emptyset
7	T_1 : Commit	Commit T_1	$\{T_1 \rightarrow T_3\}$	$\{T_1\}$
8	T_3 : Commit	Commit T_3	$\{T_1 \rightarrow T_3\}$	$\{T_1, T_3\}$
9	$T_2:(W, D, 3)$	Invalid and re-execute		
10	$T_2:(R, D, 5)$ (Re-execute)	T_2 reads D on T_1 : ($D = 5$)	$\{T_2\}$	$\{T_1, T_3\}$
11	$T_2:(W, D, 2)$	T_2 writes $D = 2$	$\{T_1 \rightarrow T_2, T_1 \rightarrow T_3\}$	$\{T_1, T_3\}$
12	T_2 : Commit	Commit T_2	$\{T_1 \rightarrow T_2, T_1 \rightarrow T_3\}$	$\{T_1, T_3, T_2\}$

Table 1: An example of generating the dependency while executing the transactions $\{T_1, T_2, T_3\}$ that access the data D and determining the execution order.

a DAG are discarded and must be resubmitted. Only transactions from the last two rounds or those excluded by the leader are affected. Clients will automatically retransmit transactions lost due to the reconfiguration.

Censorship Attacks. Malicious replicas may attempt censorship via message drops, transaction rescheduling, DDoS attacks, or proposal halting [26, 59]. As each replica governs an entire shard in Thunderbolt, such attacks can paralyze specific shards. The reconfiguration mechanism counters this by periodically reassigning shards to new replicas, limiting the impact window of compromised nodes.

7 Concurrent Executor

The concurrent executor (*CE*) is a critical component enabling Thunderbolt to process Single-shard TXs concurrently during the preplay phase. As a nondeterministic concurrency control executor, *CE* generates a serialized execution order, read/write sets, and execution results for transaction batches. These outputs allow any

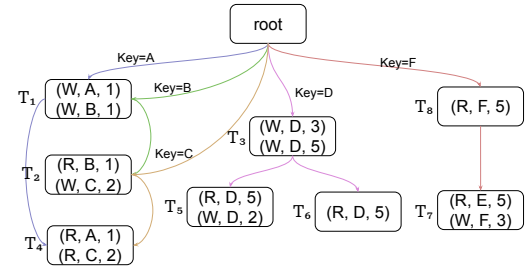


Figure 8: Dependency Graph on *Thunderbolt*. Edges with the same color represent a dependency graph with a specific key.

replica to independently verify correctness, even though the *CE*-derived order may differ from the transactions' arrival sequence.

The architecture of *CE* is illustrated in Figure 7, where a set of executors executes the transactions, and a concurrency controller (*CC*) determines the execution results among the transactions.

Transactions progress through a two-phase data flow: an execution phase (operations processing) and a finalization phase (commit/abort decisions). Table 1 exemplifies this workflow using transactions $\{T_1, T_2, T_3\}$.

7.1 Execution Phase

During the execution phase, the executors access the data within *CC* directly and *CC* maintains a dependency graph to keep track of the relationship between transactions and all the results are stored in the graph directly to avoid accessing the disk IO. The critical characteristic of *CC* is that *CC* only maintains the graph based on the current operations among the transactions without requiring any read/write sets knowledge. Furthermore, *CC* is nondeterministic and can arrange transactions in any order. For example, if two transactions T_1 and T_2 update the duplicate keys, a dependency edge between T_1 and T_2 may not be created since T_1 and T_2 can be arranged in any order in the current state.

While receiving an operation from a transaction T sent by the executors identified accessing the key K , denoted as O_k , *CC* checks the relationships among the transactions. If T conflicts with other transactions or has been aborted by other transactions, the operation O_k will not be considered valid. For instance, T_2 at time 9 in Table 1 is an example of an invalid operation, as it was aborted by T_1 at time 5 due to its outdated read in D . Transaction T will be aborted in such cases and require reexecution. Otherwise, if the operation O_k is valid, it will be added to the dependency graph (section 8.1) and obtain the operation result, such as the value V that O_k intends to read. We can obtain the operation results from other transactions directly based on the dependency graph to allow reading uncommitted data, such as T_2 reads D on T_1 at time 2.

7.2 Finalization Phase

During the finalization phase, the executor informs *CC* that the executor has completed all the operations. Then *CC* will update the results to the storage asynchronously once all its dependencies have been committed and assign the execution order to the transactions. If *CC* has terminated the transaction due to conflicts with other transactions, *CC* aborts the transaction and notifies the executor to restart the execution.

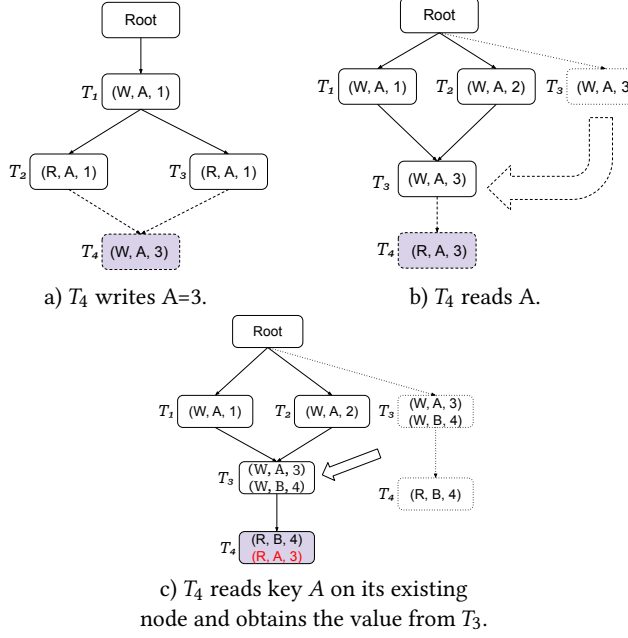


Figure 9: An example of incorporating operations into the dependency graph. The relationships between the nodes may be adjusted to ensure correctness.

8 Dependency Graph in CC

This section explains the dependency graph G , which is central to the CC component. It plays a crucial role in maintaining the causal relationships between transactions during the preplay process in CE . The CC component ensures that the sequential order of execution defined by G is valid.

8.1 Dependency Graph Construction

A Dependency Graph is a graph $G(V, E)$ that plays a crucial role in tracking the causal relationship between transactions in CC . Each node $v \in V$ represents a specific transaction. Additionally, each edge $e(u, v, k) \in E$ indicates a connection between two transactions u and v on a key K . This relationship is represented as $u \rightarrow_k v$. For example, in Figure 8, transaction T_5 generates an edge $e(T_3, T_5, D)$ from T_3 because T_5 acquires the value 3 of key D from T_3 .

Without loss of generality, we have assigned a root node denoted R and added edges $e(R, u, k) \in E$ for each $u \in V$ that accesses the key K but does not have any incoming edge on key K , such as T_7 and T_8 in Figure 8.

If the graph G is acyclic, a sequential order can be established by generating a topological order. It is crucial that every transaction must obtain the same causal order in any topological order from G to ensure consistency. Therefore, G is considered a valid graph only if any sequential order generated from the topological order is a valid serialization order and produces the same results. By following any correct order, all transactions will yield the same execution results. However, because of the nondeterministic characteristic, the results may not be the same as those executed in their arrival order.

Each node u maintains all records of the operations triggered by a transaction u , including the resulting values. Since a transaction

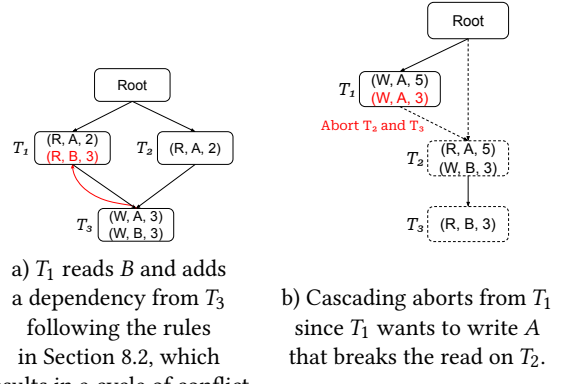


Figure 10: Cycle of conflicts and cascading aborts.

is an atomic commitment, we combine the internal operations to simplify the in-node states. However, to trace the conflicts between two nodes, we must retain the first operation if it is a read and the last operation if it is a write, to ensure that the causal relationship is not lost. Thus, we remain at most two operations in the nodes: the first read and the last write.

To help illustrate the algorithm, we define the types of each node depending on the operations it contains on a key:

- A node $v \in V$ is a read node R_v^k if the first operation on key K is a read.
- A node $v \in V$ is a write node W_v^k if v contains write operations on key K .
- The root node R is a write node.

8.2 Generating New Nodes

This section presents the process of adding operations from a new transaction to the dependency graph G .

CC creates a new node whenever an operation O_k is received from a new transaction T . If O_k is a write operation, T needs to establish a connection to each causal relation. To avoid pointing to the root and assuming that the earlier transaction will commit first, the non-write nodes v on key K , which only contains reads, without any outgoing edges (not dependent by other nodes) are selected, and edges $e(v, u, k)$ are added, pointing to u (Figure 9 (a)).

On the other hand, when a read operation is performed, CC selects the latest write node u to obtain the latest value or selects the root to read the data value from storage if no write nodes exist. If the write node u is selected, we need to make all other write nodes W_v^k contain a path to u to guarantee the correctness for the read after write between u and v . Finally, the operation and its result $\langle \text{Type}, \text{Key}, \text{Result} \rangle$ will be written into the node u . An example of adding a new read operation on A from T_4 is depicted in Figure 9 (b). T_4 selects T_3 to read to obtain $A = 3$ and adds an edge from T_3 and a record $\langle R, A, 3 \rangle$ is logged down in the node. Then T_3 will add two edges from T_1 and T_2 , respectively.

8.3 Operations on Existing Nodes

When receiving an operation O_k for the key K from an existing transaction T in G , CC will select the corresponding node u to attach the record. If O_k is a read operation, the result will be directly retrieved if u contains the record for key K . Otherwise, it will

proceed with the new node operation as specified in Section 8.2 to choose a previous one to access the value. Figure 9 (c) illustrates an instance where T_4 reads key A as its second operation and retrieves the value from T_3 . If O_k is a write operation, the operation will be appended to the node.

8.4 Conflict Detection

Appending the records to an existing node may lead to transaction conflicts. For instance, a transaction updates the value again but it has been read by another transaction or a dependency cycle is created due to the dependency on another key since we always find the latest write to retrieve the value. Figure 10 (a) depicts a scenario in which T_1 attempts to retrieve the value of B from T_3 , which has established a dependency from T_1 due to key A , which results in the creation of a dependency cycle. In this case, CC will try to read the value from its ancestor, like B reads the value from the *Root* Figure 10 (a). If there is still any conflict with other transactions, CC will trigger the abort process.

Once conflicts are detected, CC triggers an abort process as follows:

- (1) If u only contains read operations, abort T itself.
- (2) If u contains write operations, cascading abort from T .

In Figure 10 (b), we need to abort T_2 and T_3 since T_1 contains a write operation. However, in Figure 10 (a), we only need to remove T_1 and keep T_3 alive.

9 Concurrency Executor Evaluation

This section evaluates Thunderbolt by assessing its performance on the *CE* and the Thunderbolt protocol. We implement all the baseline comparisons using Apache ResilientDB (Incubating) [2, 38]. Apache ResilientDB is an open-source incubating blockchain project that supports various consensus protocols. It provides a fair comparison of each protocol by offering a high-performance framework. Researchers can focus solely on their protocols without considering system structures such as the network and thread models.

We will begin by comparing *CE* with two baseline protocols: *OCC* [51] and *2PL-No-WAIT* [80]. Additionally, we will analyze the performance of Thunderbolt, which is built on *Tusk* [23], and we will also use *Tusk* as a baseline for our comparisons. For our input workload, we will utilize *SmallBank* [1, 6], a benchmarking suite that simulates common asset transfer transactions. This suite is also used to evaluate variant block systems [34, 53, 56, 65, 73, 88, 106].

9.1 Baseline Protocols

We implement *OCC* [51] and *2PL-No-WAIT* [101, 102] to compare the performance against our concurrent executor. We set up our experiments on AWS c5.9xlarge consisting of 36 vCPU, 72GB of DDR3 memory. We use *LevelDB* as the storage to save the balance of each account.

OCC. Each executor is responsible for locally executing transactions. When an operation within a transaction T requires reading the value of a key K that the executor has not previously accessed during the execution, the executor will retrieve the value from the storage. Each value also contains a version to indicate the time the value was obtained. Any write operation will update the values locally. Upon completion of T , all the updated values will be

forwarded to a central verifier. The verifier will cross-check the value versions by comparing them with the current versions in the storage. If there is a mismatch, the commit will be rejected, necessitating the re-execution of T .

2PL-No-WAIT. Each executor performs transactions by directly accessing the storage through a central controller. When an operation within a transaction T requires the read or update of a key K , the controller will lock K to prevent conflicts. If an operation seeks to access K but discovers that another executor has locked it, the executor will release all locks and re-execute T . Upon the completion of T , all the results will be transmitted to storage, and all locks will be released.

9.2 Experiment Setup With Smallbank

SmallBank [1] is a transactional system that comprises six distinct transaction types, five of which are designed to update account balances, while the remaining transaction is a read-only query that retrieves both checking and saving the account details of a user. Our focus is on two types of transactions: *SendPayment* and *GetBalance*, which are used to transfer funds between two accounts and retrieve account balances, respectively. Our objective is to evaluate the performance under varying read-write balance workloads. During a *SendPayment* transaction, the account balances are updated by reading the current balance and then writing the new values back. We created 10,000 accounts and conducted each experiment 50 times to obtain the average outputs.

We evaluated the impact of parallel execution. We measured the performance by uniformly selecting *GetBalance* with a probability of P_r while *SendPayment* with $1 - P_r$. We follow a Zipfian distribution to select accounts as transaction parameters and set the Zipfian parameter θ . The value of θ determines the level of account contention, with higher values leading to higher contention. We focus only on data workloads with high contention by setting $\theta = 0.85$.

9.3 Impact from Concurrent Executor

We first evaluate the impact of increasing the number of executors to execute the transactions, then measure the aborts produced by each protocol. We ran two batch sizes $b300$ and $b500$ for each protocol: *Thunderbolt-b300*, *Thunderbolt-b500*, *OCC-b300*, *OCC-b500*, *2PL-No-WAIT-b300*, and *2PL-No-WAIT-b500*. We set $P_r = 0.5$ to measure a read-write balanced workflow and $P_r = 0$ on an update-only workflow.

Number of Executors. In the read-write balanced workflow, the results depicted in Figure 11 (a) show that *2PL-No-WAIT* protocols with different batch sizes all experience a performance drop when increasing the number of executors beyond 8. However, *Thunderbolt* and *OCC* protocols with all the batch sizes obtain their highest throughputs on 12 executors and maintain stable throughput. *Thunderbolt-b500* obtained 43K TPS while *OCC-b500* achieved 35K TPS.

In the update-only workflow, the results shown in Figure 11 (b) indicate that *OCC* and *2PL-No-WAIT* stopped increasing earlier in 4 executors (both around 22K TPS) while *Thunderbolt* provides a peak throughput (28K TPS) in 12 executors.

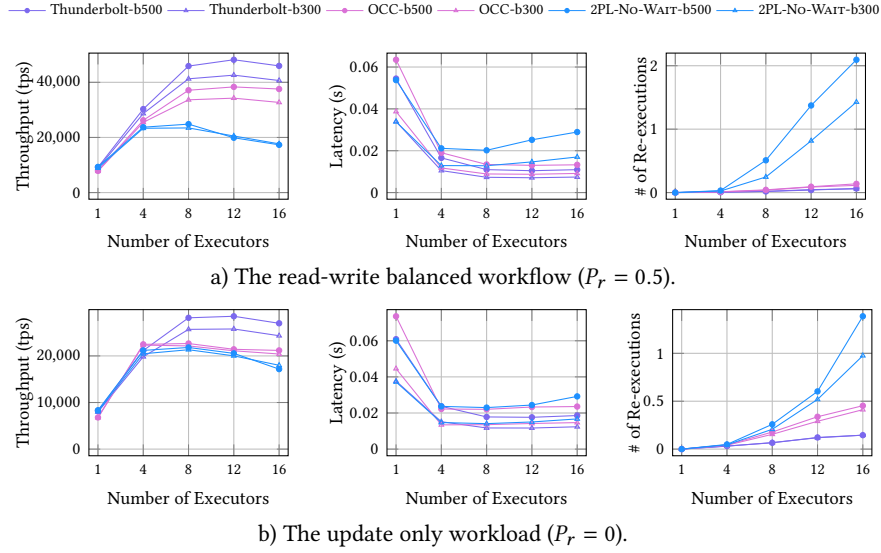


Figure 11: Evaluation of CE on different numbers of executors.

These experiments demonstrate that all the protocols do not obtain significant benefits for a large number of executors in a high-competition workflow. However, Thunderbolt can still achieve more parallelism with more executors.

Evaluation of Abort Rates. As we increased the number of executors, we also measured the average number of re-executions for the transactions. The results in Figure 11 indicate that when the number of executors goes beyond 8, all 2PL-No-WAIT protocols experience a significant increase in the rate of abortions, leading to a drop in throughput from 24k to 18k in the read-write balanced workflow. While OCC protocols provide a lower rate within the read-write balanced workflow. However, Thunderbolt achieves the lowest abortions, with Thunderbolt-b500 reducing 50% of the abortions from OCC-b500 and 90% from 2PL-No-WAIT-b500 in all the experiments.

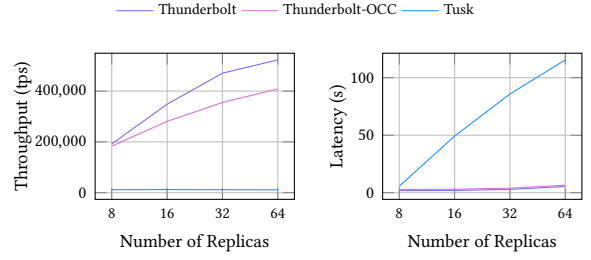
10 System Evaluation

We conducted evaluations to determine the impact of Thunderbolt built on Tusk. In our evaluation, we compared the performance of Thunderbolt with Tusk, which executes transactions in order after reaching a total order after DAG protocols. We evaluated the impact of different components of the protocol by comparing the results between three systems:

- Thunderbolt: Leverage CE + parallel verification.
- Thunderbolt-OCC: Combine OCC + parallel verification.
- Tusk: Utilize the OE model.

As the serialized verification will execute the transactions in order to verify the results, we will expect that any DAG-based protocols with serialized verification will provide the same behavior with Tusk. We also leveraged SmallBank as the input workload.

Each replica was configured with CE comprising 16 executors to process transaction batches of 500, alongside 16 validators to verify blocks post-consensus. We scaled the system from 8 to 64 replicas. By default, K' was set to a sufficiently large value to disable shard rotation. In the final phase of our evaluation, we examined the

Figure 12: Throughput and average latency within different replicas within $P_r = 0.5$.

impact of varying K' values, which govern the frequency of shard reconfiguration (Section 10).

SmallBank. In the SmallBank workload experiments, we focused on a read-write balanced scenario ($P_r = 0.5$), where half of the transactions are read-only. Transaction addresses were selected from a pool of 1000 users with a skew parameter $\theta = 0.85$ to simulate a high-contention workload.

The results, as shown in Figure 12, demonstrate that Thunderbolt significantly outperformed Tusk's sequential execution model, achieving a 50x speedup. Specifically, Thunderbolt reached 500K TPS with 64 replicas, compared to Tusk's 11K TPS. This improvement highlights the benefits of executing transactions in parallel.

We also compared Thunderbolt with Thunderbolt-OCC, which replaces the CE with OCC. While Thunderbolt-OCC matched Thunderbolt's throughput at 8 replicas, it lagged behind at scale, achieving only 400K TPS with 64 replicas. Furthermore, Thunderbolt maintained a low transaction latency of 5 seconds, whereas Tusk's latency soared to 100 seconds under the same conditions.

Cross-shard Transactions. Next, we evaluated the impact of Cross-shard TXs using 16 replicas. We randomly assigned a percentage $P\%$

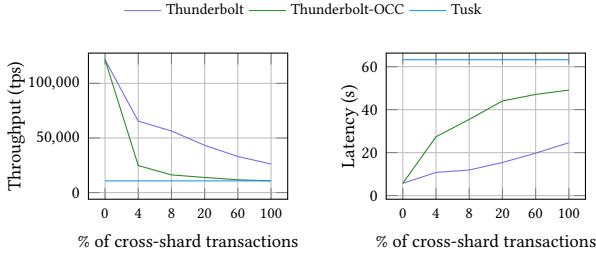


Figure 13: Throughput and average latency within different ratios of cross-shard transactions within 16 replicas.

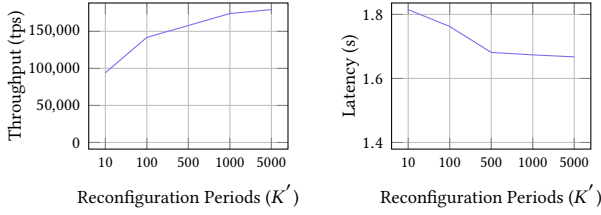


Figure 14: Throughput and average latency within different reconfiguration periods within 8 replicas.

($0 < P \leq 100$) of transactions to be processed by two shards. Additionally, we assessed the benefits of parallel execution by comparing Thunderbolt-OCC.

As shown in Figure 13, the performance of both Thunderbolt and Thunderbolt-OCC declined as the percentage P increased. In scenarios with only single-shard transactions ($P = 0$), both systems achieved 100K TPS. However, when P increased to 8%, Thunderbolt-OCC's throughput dropped to 16K TPS, while Thunderbolt maintained a significantly higher throughput of 64K TPS. Thunderbolt-OCC's performance aligned closely with Tusk, achieving approximately 10K TPS. In contrast, Thunderbolt delivered 19K TPS even when all transactions were cross-shard, demonstrating the advantages of its parallel execution model and nondeterministic ordering on *CE*.

Latency metrics further highlighted Thunderbolt's superiority. Under high-contention workloads, Thunderbolt achieved a transaction latency of 24s seconds, while Thunderbolt-OCC's latency was nearly double at 50 seconds.

Reconfiguration Periods. Now, we analyze the performance using different reconfiguration periods K' to transition the shard submitters into a new DAG on 8 replicas. Figure 14 demonstrates that Thunderbolt exhibited lower performance with smaller K' values (80K TPS with $K' = 10$), attributed to the costly transition between DAGs. Conversely, when K' was increased to over 1000, Thunderbolt demonstrated significantly improved stability, achieving a throughput of 180K TPS. Additionally, the average latency decreased from 1.9s to 1.7s as K' increased from 10 to 5000. Figure 15 also shows the average run time of committing proposals per 100 rounds, that is $\frac{1}{100} \sum (T_{commit(i)} - T_{commit(i-1)})$ where $T_{commit(i)}$ is the time of committing round i . We set K' as 300 and it was demonstrated that Thunderbolt will not get stuck during the reconfiguration. The runtime of each round is around 0.07s to 0.1s.

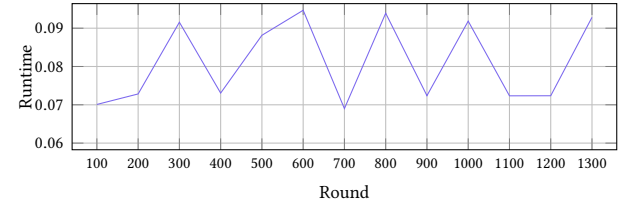


Figure 15: Average latency per 100 rounds and reconfigure the shard per 300 rounds.

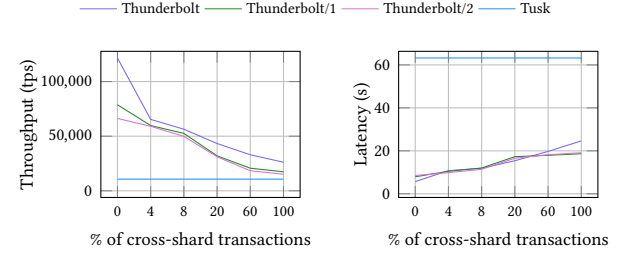


Figure 16: Throughput and average latency within different ratios of cross-shard transactions within 16 replicas when f ($f = 1$ or $f = 2$) replicas failed.

Failures. Finally, we evaluated the impact of replica failures within 16 replicas. We forced f replicas ($f = 1$ or $f = 2$) to stop working during the experiments. We randomly designated a percentage P ($0 < P \leq 100$) of the transactions to be processed by two shards.

Figure 16 reveals that Thunderbolt still can provide higher throughputs when some shards stop working. When one replica failed to propose transactions, Thunderbolt

1 ($f = 1$) obtained 78K TPS working on all Single-shard TXs ($P = 0$) and 17K TPS on all Cross-shard TXs while when two replicas failed to propose transactions, Thunderbolt

2 ($f = 2$) obtained 66K TPS on all Single-shard TXs and 15K TPS on all Cross-shard TXs. However, the results show that the latency remains stable even if some replicas fail to process, benefiting from the leader rotation of the DAG protocols.

11 Related work

11.1 Sharding on DAG-based protocol

Numerous studies [4, 24, 39, 42, 50, 70, 91, 104] have highlighted the need for sharding to enhance scalability in blockchain systems. Directed Acyclic Graph (DAG)-based blockchains [11, 12, 14, 22, 23, 48, 49, 55, 57, 71, 79, 82–84, 96, 100] offer an alternative for improving concurrent transaction processing through the DAG data structure. Systems like BullShark [83], Tusk [23], and DAG-Rider [48] separate transaction dissemination from ordering, achieving high throughput and rapid confirmation. Nezha [95] investigates address-based dependencies for conflict detection and proposes a concurrent transaction processing mechanism for DAG-based blockchains.

Few approaches, however, provide sharding strategies for DAG protocols. BrokerChain [45] and SharDAG [21] utilize account-based protocols to achieve eventual atomicity through incentive mechanisms. BrokerChain employs brokers with accounts across

multiple shards for cross-shard transactions, while SharDAG introduces avatar accounts—temporary accounts derived from a primary account—used within each shard. These avatar accounts are aggregated back to the primary account to facilitate efficient cross-shard transactions. The Two-Phase Commit (2PC) method is also used to ensure atomicity in cross-shard transactions [24, 44]. Sharper [8] and DAG-BLOCK [68] implement multi-shard consensus, but these methods incur delays due to additional cross-shard communications.

In contrast, Thunderbolt designates each replica as a shard leader, leveraging the DAG to manage both single-shard and cross-shard transactions without coordinators or external mechanisms, and does not rely on account-based information.

11.2 Execute-Order-Validate

The Execute-Order-Validate (EOX) framework was originally introduced by Hyperledger Fabric [10] offering the advantage of allowing transactions to be optimistically executed by a subset of executors before obtaining a global order. However, parallel execution may lead to conflicts between two transactions, causing validation to abort the transactions after being ordered.

Various techniques have been proposed to improve the bottleneck on Hyperledger Fabric, including optimizing the peer process, replacing the state DB with a hash table, and pipelining the execution [34, 89, 90]. Other platforms like Fabric++ [75], XOXFabric [33], and FabricSharp [73] have also been developed to reorder transactions within a block by analyzing their dependencies after consensus, which reduces the abort rate.

Thunderbolt, inspired by Hyperledger Fabric, has implemented an execution model that allows transactions to be executed before ordering. However, unlike Hyperledger, Thunderbolt distributes transactions in different shards, and transactions in each shard will be executed by a shard leader. This approach enables each shard leader to leverage the concurrent executor to execute transactions in parallel while also reordering them to improve performance and reduce abort rates.

11.3 Concurrent Execution

Deterministic approaches [29, 67, 98] have been proposed to enhance transaction execution efficiency by developing a dependency graph that enables concurrent execution while minimizing conflicts. Techniques such as Transaction Chopping [76, 77], SChain [20], and Caracal [69] further this concept by segmenting transactions into smaller components prior to graph construction. Additionally, the use of non-volatile main memory [92] has been suggested to address challenges posed by long-latency transactions.

CHIRON [64] employs BlockSTM [32], which facilitates non-deterministic execution to extract dependencies from smart contracts on the Ethereum platform, thereby improving performance for both straggling and full nodes. BlockSTM allows for parallel execution of smart contracts, with the execution order determined by transaction arrival times, producing corresponding read and write sets.

In contrast, Thunderbolt does not depend on arrival times or read/write set information for transaction processing. Instead, it dynamically assigns execution order to minimize transaction conflicts.

11.4 Transaction Reordering

BCC [103] introduced a method aimed at minimizing the number of aborted transactions by adjusting the commit order based on commit times. In the study presented in [25], a directed graph is constructed within a batch, and a greedy algorithm is used to reorder transactions, effectively addressing the NP-hard problem encountered in highly contentious scenarios. Similar methodologies have been explored in [33, 73, 75]. However, it is essential to note that these approaches often increase latency as they seek to identify the optimal global order from a deterministic graph derived from the read/write sets obtained during execution.

In contrast, Thunderbolt adopts a more dynamic approach by constructing and maintaining the graph in real-time. This strategy ensures that the graph remains up-to-date, allowing adjustments to the transaction order to achieve the desired results.

11.5 Concurrent Consensus

A high-performance and scalable blockchain framework is vital to implement real-world applications [9, 35, 37, 74]. PoE [36] improves the Practical Byzantine Fault Tolerance protocol (PBFT) [19] by incorporating speculative execution to streamline the process. Furthermore, protocols such as RCC [38], FlexiTrust [40], and SpotLess [47] enhance the effectiveness of single-leader systems by integrating multiple leaders to increase parallelism. However, it is important to note that these protocols do not support reconfiguration.

12 Conclusions

We present Thunderbolt, an innovative sharding system designed to optimize smart contract execution through the integration of the Order-Execute and Execute-Order-Validate models. Thunderbolt efficiently distributes transactions across multiple shards and employs Directed Acyclic Graph (DAG)-based protocols to enable seamless transaction propagation among all shards.

In our framework, Single-shard TXs are processed prior to consensus, whereas Cross-shard TXs are executed following the consensus process. To maintain consistency between single-shard and cross-shard transactions, Thunderbolt utilizes deterministic leaders within the DAG architecture. Additionally, we have developed a concurrent executor that significantly enhances the performance of Single-shard TXs by dynamically constructing a dependency graph, eliminating the necessity for pre-existing knowledge of read/write sets.

A key feature of Thunderbolt is its ability to leverage the inherent properties of the DAG to facilitate a nonblocking transition to a new DAG structure. This allows for the rotation of submitters for each shard in the event of detecting a malicious submitter. Our performance evaluations demonstrate that Thunderbolt achieves an impressive speedup of up to 50x compared to the native execution provided by Tusk.

Artifact Availability:

The source code, data, and/or other artifacts have been made available at <https://github.com/apache/incubator-resilientdb/tree/Thunderbolt>.

References

- [1] 2019. smallbank benchmark. <http://hstore.cs.brown.edu/documentation/deployment/benchmarks/smallbank/>
- [2] 2024. Apache ResilientDB (Incubating). <https://resilientdb.incubator.apache.org/>
- [3] Rakesh Agrawal, Michael J Carey, and Miron Livny. 1987. Concurrency control performance modeling: Alternatives and implications. *ACM Transactions on Database Systems (TODS)* 12, 4 (1987), 609–654.
- [4] Mustafa Al-Bassam, Alberto Sonnino, Shehar Bano, Dave Hrycyszyn, and George Danezis. 2017. Chainspace: A sharded smart contracts platform. *arXiv preprint arXiv:1708.03778* (2017).
- [5] Amjad Aldweesh, Maher Alharby, Maryam Mehrnezhad, and Aad Van Moorsel. 2019. OpBench: A CPU performance benchmark for Ethereum smart contract operation code. In *2019 IEEE International Conference on Blockchain (Blockchain)*. IEEE, 274–281.
- [6] Mohammad Alomari, Michael Cahill, Alan Fekete, and Uwe Rohm. 2008. The cost of serializability on platforms that use snapshot isolation. In *2008 IEEE 24th International Conference on Data Engineering*. IEEE, 576–585.
- [7] Mohammad Javad Amiri, Divyakant Agrawal, and Amr El Abbadi. 2019. Caper: a cross-application permissioned blockchain. *Proceedings of the VLDB Endowment* 12, 11 (2019), 1385–1398.
- [8] Mohammad Javad Amiri, Divyakant Agrawal, and Amr El Abbadi. 2021. Sharper: Sharding permissioned blockchains over network clusters. In *Proceedings of the 2021 international conference on management of data*. 76–88.
- [9] Mohammad Javad Amiri, Chenyuan Wu, Divyakant Agrawal, Amr El Abbadi, Boon That Loo, and Mohammad Sadoghi. 2022. The Bedrock of BFT: A Unified Platform for BFT Protocol Design and Implementation. *CoRR* abs/2205.04534 (2022). <https://doi.org/10.48550/arXiv.2205.04534> arXiv:2205.04534
- [10] Elli Androulaki, Artem Barger, Vito Bortnikov, Christian Cachin, Konstantinos Christidis, Angelo De Caro, David Enyeart, Christopher Ferris, Gennady Laventman, Yacov Manevich, Srinivasan Muralidharan, Chet Murthy, Binh Nguyen, Manish Sethi, Gari Singh, Keith Smith, Alessandro Sorniotti, Chrysoula Stathakopoulou, Marko Vukolić, Sharon Weed Cocco, and Jason Yellick. 2018. Hyperledger Fabric: A Distributed Operating System for Permissioned Blockchains. In *Proceedings of the Thirteenth EuroSys Conference*. ACM, 30:1–30:15. <https://doi.org/10.1145/3190508.3190538>
- [11] Balaji Arun, Zekun Li, Florian Suri-Payer, Sourav Das, and Alexander Spiegelman. 2024. Shoal++: High Throughput DAG BFT Can Be Fast! *arXiv preprint arXiv:2405.20488* (2024).
- [12] Kushal Babel, Andrey Chursin, George Danezis, Lefteris Kokoris-Kogias, and Alberto Sonnino. 2023. Mysticeti: Low-latency dag consensus with fast commit path. *arXiv preprint arXiv:2310.14821* (2023).
- [13] Kushal Babel, Andrey Chursin, George Danezis, Lefteris Kokoris-Kogias, and Alberto Sonnino. 2023. Mysticeti: Low-Latency DAG Consensus with Fast Commit Path. *arXiv preprint arXiv:2310.14821* (2023).
- [14] Leemon Baird. 2016. The swirls hashgraph consensus algorithm: Fair, fast, byzantine fault tolerance. *Swirls Tech Reports SWIRLDS-TR-2016-01, Tech. Rep* 34 (2016), 9–11.
- [15] Sam Blackshear, Andrey Chursin, George Danezis, Anastasios Kichidis, Lefteris Kokoris-Kogias, Xun Li, Mark Logan, Ashok Menon, Todd Nowacki, Alberto Sonnino, et al. 2023. Sui ltritis: A blockchain combining broadcast and consensus. *arXiv preprint arXiv:2310.18042* (2023).
- [16] Dan Boneh, Ben Lynn, and Hovav Shacham. 2001. Short signatures from the Weil pairing. In *International conference on the theory and application of cryptology and information security*. Springer, 514–532.
- [17] Vitalik Buterin et al. 2014. A next-generation smart contract and decentralized application platform. *white paper* 3, 37 (2014), 2–1.
- [18] Michael Casey, Jonah Crane, Gary Gensler, Simon Johnson, and Neha Narula. 2018. The impact of blockchain technology on finance: A catalyst for change. (2018).
- [19] Miguel Castro and Barbara Liskov. 2002. Practical Byzantine Fault Tolerance and Proactive Recovery. *ACM Trans. Comput. Syst.* 20, 4 (2002), 398–461. <https://doi.org/10.1145/571637.571640>
- [20] Zhihao Chen, Haizhen Zhuo, Quanqing Xu, Xiaodong Qi, Chengyu Zhu, Zhao Zhang, Cheqing Jin, Aoying Zhou, Ying Yan, and Hui Zhang. 2021. SChain: a scalable consortium blockchain exploiting intra-and inter-block concurrency. *Proceedings of the VLDB Endowment* 14, 12 (2021), 2799–2802.
- [21] Feng Cheng, Jiang Xiao, Cunyang Liu, Shijie Zhang, Yifan Zhou, Bo Li, Baochun Li, and Hai Jin. 2024. Shardag: Scaling dag-based blockchains via adaptive sharding. In *2024 IEEE 40th International Conference on Data Engineering (ICDE)*. IEEE, 2068–2081.
- [22] Anton Chryumov. 2016. Byteball: A decentralized system for storage and transfer of value. URL <https://byteball.org/Byteball.pdf> (2016), 11.
- [23] George Danezis, Lefteris Kokoris-Kogias, Alberto Sonnino, and Alexander Spiegelman. 2022. Narwhal and Tusk: A DAG-Based Mempool and Efficient BFT Consensus. In *Proceedings of the Seventeenth European Conference on Computer Systems*. Association for Computing Machinery, New York, NY, USA, 34–50.
- [24] Hung Dang, Tien Tuan Anh Dinh, Dumitrel Loghin, Ee-Chien Chang, Qian Lin, and Beng Chin Ooi. 2019. Towards scaling blockchain systems via sharding. In *Proceedings of the 2019 international conference on management of data*. 123–140.
- [25] Baili Ding, Luca Kot, and Johannes Gehrke. 2018. Improving optimistic concurrency control through transaction batching and operation reordering. *Proceedings of the VLDB Endowment* 12, 2 (2018), 169–182.
- [26] Christos Douligeris and Aikaterini Mitrokotsa. 2004. DDoS attacks and defense mechanisms: classification and state-of-the-art. *Computer networks* 44, 5 (2004), 643–666.
- [27] Cynthia Dwork, Nancy Lynch, and Larry Stockmeyer. 1988. Consensus in the presence of partial synchrony. *Journal of the ACM (JACM)* 35, 2 (1988), 288–323.
- [28] Muhammad El-Hindi, Carsten Binnig, Arvind Arasu, Donald Kossmann, and Ravi Ramamurthy. 2019. BlockchainDB: A shared database on blockchains. *Proceedings of the VLDB Endowment* 12, 11 (2019), 1597–1609.
- [29] Jose M Faleiro, Daniel J Abadi, and Joseph M Hellerstein. 2017. High performance transactions via early write visibility. *Proceedings of the VLDB Endowment* 10, 5 (2017).
- [30] Peter Franaszek and John T Robinson. 1985. Limitations of concurrency in transaction processing. *ACM Transactions on Database Systems (TODS)* 10, 1 (1985), 1–28.
- [31] Lan Ge, Christopher Brewster, Jacco Spek, Anton Smeenk, Jan Top, Frans Van Diepen, Bob Klasee, Conny Graumanns, and Marieke de Ruyter de Wildt. 2017. *Blockchain for agriculture and food: Findings from the pilot study*. Number 2017–112. Wageningen Economic Research.
- [32] Rati Gelashvili, Alexander Spiegelman, Zhuolun Xiang, George Danezis, Zekun Li, Dahlia Malkhi, Yu Xia, and Runtian Zhou. 2023. Block-stm: Scaling blockchain execution by turning ordering curse to a performance blessing. In *Proceedings of the 28th ACM SIGPLAN Annual Symposium on Principles and Practice of Parallel Programming*. 232–244.
- [33] Christian Gorenflo, Lukasz Golab, and Srinivasan Keshav. 2020. XOX Fabric: A hybrid approach to blockchain transaction execution. In *2020 IEEE International Conference on Blockchain and Cryptocurrency (ICBC)*. IEEE, 1–9.
- [34] Christian Gorenflo, Stephen Lee, Lukasz Golab, and Srinivasan Keshav. 2020. FastFabric: Scaling hyperledger fabric to 20 000 transactions per second. *International Journal of Network Management* 30, 5 (2020), e2099.
- [35] Suyash Gupta, Mohammad Javad Amiri, and Mohammad Sadoghi. 2023. Chemistry behind Agreement. In *13th Conference on Innovative Data Systems Research, CIDR 2023, Amsterdam, The Netherlands, January 8–11, 2023*. www.cidrdb.org.
- [36] Suyash Gupta, Jelle Hellings, Sajjad Rahnama, and Mohammad Sadoghi. 2021. Proof-of-Execution: Reaching Consensus through Fault-Tolerant Speculation. In *Proceedings of the 24th International Conference on Extending Database Technology*.
- [37] Suyash Gupta, Jelle Hellings, and Mohammad Sadoghi. 2021. *Fault-Tolerant Distributed Transactions on Blockchain*. Morgan & Claypool Publishers. (2021).
- [38] Suyash Gupta, Jelle Hellings, and Mohammad Sadoghi. 2021. RCC: Resilient Concurrent Consensus for High-Throughput Secure Transaction Processing. In *37th IEEE International Conference on Data Engineering, ICDE 2021, Chania, Greece, April 19–22, 2021*. IEEE, 1392–1403. <https://doi.org/10.1109/ICDE51399.2021.00124>
- [39] Suyash Gupta, Sajjad Rahnama, Jelle Hellings, and Mohammad Sadoghi. 2020. ResilientDB: Global Scale Resilient Blockchain Fabric. *Proc. VLDB Endow.* 13, 6 (2020), 868–883. <https://doi.org/10.14778/3380750.3380757>
- [40] Suyash Gupta, Sajjad Rahnama, Shubham Pandey, Natacha Crooks, and Mohammad Sadoghi. 2023. Dissecting BFT Consensus: In Trusted Components we Trust!. In *Proceedings of the Eighteenth European Conference on Computer Systems, EuroSys 2023, Rome, Italy, May 8–12, 2023*. Giuseppe Antonio Di Luna, Leonardo Querzoni, Alexandra Fedorova, and Dushyanth Narayanan (Eds.). ACM, 521–539.
- [41] Suyash Gupta, Sajjad Rahnama, and Mohammad Sadoghi. 2020. Permissioned blockchain through the looking glass: Architectural and implementation lessons learned. In *2020 IEEE 40th International Conference on Distributed Computing Systems (ICDCS)*. IEEE, 754–764.
- [42] Jelle Hellings and Mohammad Sadoghi. 2023. ByShard: sharding in a Byzantine environment. *VLDB J.* 32, 6 (2023), 1343–1367.
- [43] Maurice Herlihy. 2019. Blockchains from a distributed computing perspective. *Commun. ACM* 62, 2 (2019), 78–85.
- [44] Zicong Hong, Song Guo, and Peng Li. 2022. Scaling blockchain via layered sharding. *IEEE Journal on Selected Areas in Communications* 40, 12 (2022), 3575–3588.
- [45] Huawei Huang, Xiaowen Peng, Jianzhou Zhan, Shenyang Zhang, Yue Lin, Zibin Zheng, and Song Guo. 2022. Brokerchain: A cross-shard blockchain protocol for account/balance-based state sharding. In *IEEE INFOCOM 2022–IEEE Conference on Computer Communications*. IEEE, 1968–1977.
- [46] Maged N Kamel Boulos, James T Wilson, and Kevin A Clauson. 2018. Geospatial blockchain: promises, challenges, and scenarios in health and healthcare. , 10 pages.

[47] Dakai Kang, Sajjad Rahnama, Jelle Hellings, and Mohammad Sadoghi. 2024. SpotLess: Concurrent Rotational Consensus Made Practical through Rapid View Synchronization. In *40th IEEE International Conference on Data Engineering, ICDE 2024, Utrecht, Netherlands, May 13-17, 2024*. IEEE.

[48] Idit Keidar, Eleftherios Kokoris-Kogias, Oded Naor, and Alexander Spiegelman. 2021. All you need is dag. In *Proceedings of the 2021 ACM Symposium on Principles of Distributed Computing*. 165–175.

[49] Idit Keidar, Oded Naor, Ouri Poupko, and Ehud Shapiro. 2022. Cordial miners: Fast and efficient consensus for every eventuality. *arXiv preprint arXiv:2205.09174* (2022).

[50] Eleftherios Kokoris-Kogias, Philipp Jovanovic, Linus Gasser, Nicolas Gailly, Ewa Syta, and Bryan Ford. 2018. Omnidledger: A secure, scale-out, decentralized ledger via sharding. In *2018 IEEE symposium on security and privacy (SP)*. IEEE, 583–598.

[51] Hsiang-Tsung Kung and John T Robinson. 1981. On optimistic methods for concurrency control. *ACM Transactions on Database Systems (TODS)* 6, 2 (1981), 213–226.

[52] Satpal Singh Kushwaha, Sandeep Joshi, Dilbag Singh, Manjit Kaur, and Heung-No Lee. 2022. Ethereum smart contract analysis tools: A systematic review. *IEEE Access* 10 (2022), 57037–57062.

[53] Ziliang Lai, Chris Liu, and Eric Lo. 2023. When private blockchain meets deterministic database. *Proceedings of the ACM on Management of Data* 1, 1 (2023), 1–28.

[54] Leslie Lamport. 2019. Time, clocks, and the ordering of events in a distributed system. In *Concurrency: the Works of Leslie Lamport*. 179–196.

[55] Chenxin Li, Peilun Li, Dong Zhou, Zhe Yang, Ming Wu, Guang Yang, Wei Xu, Fan Long, and Andrew Chi-Chih Yao. 2020. A decentralized blockchain with high throughput and fast confirmation. In *2020 {USENIX} Annual Technical Conference ({USENIX} {ATC} 20)*. 515–528.

[56] Mingxuan Li, Yazhe Wang, Shuai Ma, Chao Liu, Dongdong Huo, Yu Wang, and Zhen Xu. 2023. Auto-tuning with reinforcement learning for permissioned blockchain systems. *Proceedings of the VLDB Endowment* 16, 5 (2023), 1000–1012.

[57] Dahlia Malkhi, Chrysoula Stathakopoulou, and Maofan Yin. 2023. BBCA-CHAIN: One-Message, Low Latency BFT Consensus on a DAG. *arXiv preprint arXiv:2310.06335* (2023).

[58] Microsoft. [n. d.]. eEVM. <https://github.com/microsoft/eEVM>

[59] Jelena Mirkovic and Peter Reiher. 2004. A taxonomy of DDoS attack and DDoS defense mechanisms. *ACM SIGCOMM Computer Communication Review* 34, 2 (2004), 39–53.

[60] Satoshi Nakamoto. 2009. Bitcoin: A Peer-to-Peer Electronic Cash System. <https://bitcoint.org/bitcoin.pdf>

[61] Arvind Narayanan and Jeremy Clark. 2017. Bitcoin's academic pedigree. *Commun. ACM* 60, 12 (2017), 36–45.

[62] Senthil Nathan, Chander Govindarajan, Adarsh Saraf, Manish Sethi, and Praveen Jayachandran. 2019. Blockchain meets database: Design and implementation of a blockchain relational database. *arXiv preprint arXiv:1903.01919* (2019).

[63] Faisal Nawab and Mohammad Sadoghi. 2019. Blockplane: A global-scale byzantizing middleware. In *2019 IEEE 35th International Conference on Data Engineering (ICDE)*. IEEE, 124–135.

[64] Ray Neiheiser, Arman Babaei, Giannis Alexopoulos, Marios Kogias, and Eleftherios Kokoris Kogias. 2024. CHIRON: Accelerating Node Synchronization without Security Trade-offs in Distributed Ledgers. *arXiv preprint arXiv:2401.14278* (2024).

[65] Zeshun Peng, Yanfeng Zhang, Qian Xu, Haixu Liu, Yuxiao Gao, Xiaohua Li, and Ge Yu. 2022. Neuchain: a fast permissioned blockchain system with deterministic ordering. *Proceedings of the VLDB Endowment* 15, 11 (2022), 2585–2598.

[66] Michael Pisa and Matt Juden. 2017. Blockchain and economic development: Hype vs. reality. *Center for global development policy paper* 107, 150 (2017), 1–42.

[67] Thamir M Qadah and Mohammad Sadoghi. 2018. Quecc: A queue-oriented, control-free concurrency architecture. In *Proceedings of the 19th International Middleware Conference*. 13–25.

[68] Naina Qi, Yong Yuan, and Fei-Yue Wang. 2022. DAG-BLOCK: A novel architecture for scaling blockchain-enabled cryptocurrencies. *IEEE Transactions on Computational Social Systems* 11, 1 (2022), 378–388.

[69] Dai Qin, Angela Demke Brown, and Ashvin Goel. 2021. Caracal: Contention management with deterministic concurrency control. In *Proceedings of the ACM SIGOPS 28th Symposium on Operating Systems Principles*. 180–194.

[70] Sajjad Rahnama, Suyash Gupta, Rohan Sogani, Dhruv Krishnan, and Mohammad Sadoghi. 2022. RingBFT: Resilient Consensus over Sharded Ring Topology. In *Proceedings of the 25th International Conference on Extending Database Technology*. OpenProceedings.org, 2:298–2:311. <https://doi.org/10.48786/edbt.2022.17>

[71] Mayank Raikwar, Nikita Polyanskii, and Sebastian Müller. 2024. SoK: DAG-based Consensus Protocols. In *2024 IEEE International Conference on Blockchain and Cryptocurrency (ICBC)*. IEEE, 1–18.

[72] Rasmus V Rasmussen and Michael A Trick. 2008. Round robin scheduling—a survey. *European Journal of Operational Research* 188, 3 (2008), 617–636.

[73] Pingcheng Ruan, Dumitrel Loghin, Quang-Trung Ta, Meihui Zhang, Gang Chen, and Beng Chin Ooi. 2020. A transactional perspective on execute-order-validate blockchains. In *Proceedings of the 2020 ACM SIGMOD International Conference on Management of Data*. 543–557.

[74] Mohammad Sadoghi and Spyros Blanas. 2019. *Transaction Processing on Modern Hardware*. Morgan & Claypool Publishers. <https://doi.org/10.2200/S00896ED1V01Y201901DTM058>

[75] Ankur Sharma, Felix Martin Schuhknecht, Divya Agrawal, and Jens Dittrich. 2019. Blurring the lines between blockchains and database systems: the case of hyperledger fabric. In *Proceedings of the 2019 International Conference on Management of Data*. 105–122.

[76] Dennis Shasha, Francois Llibrat, Eric Simon, and Patrick Valduriez. 1995. Transaction chopping: Algorithms and performance studies. *ACM Transactions on Database Systems (TODS)* 20, 3 (1995), 325–363.

[77] Dennis Shasha, Eric Simon, and Patrick Valduriez. 1992. Simple rational guidance for chopping up transactions. In *Proceedings of the 1992 ACM SIGMOD International Conference on management of Data*. 298–307.

[78] Madhavapeddi Shreedhar and George Varghese. 1995. Efficient fair queuing using deficit round robin. In *Proceedings of the conference on Applications, technologies, architectures, and protocols for computer communication*. 231–242.

[79] Nibesh Shrestha, Rohan Shrothrium, Aniket Kate, and Kartik Nayak. 2024. Sailfish: Towards Improving Latency of DAG-based BFT. *Cryptography ePrint Archive* (2024).

[80] Eljas Soisalon-Soininen and Tatu Ylönen. 1995. Partial strictness in two-phase locking. In *International Conference on Database Theory*. Springer, 139–147.

[81] Alberto Sonnino, Shehar Bano, Mustafa Al-Bassam, and George Danezis. 2020. Replay attacks and defenses against cross-shard consensus in sharded distributed ledgers. In *2020 IEEE European Symposium on Security and Privacy (EuroS&P)*. IEEE, 294–308.

[82] Alexander Spiegelman, Balaji Aurn, Rati Gelashvili, and Zekun Li. 2023. Shoal: Improving dag-bft latency and robustness. *arXiv preprint arXiv:2306.03058* (2023).

[83] Alexander Spiegelman, Neil Giridharan, Alberto Sonnino, and Lefteris Kokoris-Kogias. 2022. Bullshark: Dag bft protocols made practical. In *Proceedings of the 2022 ACM SIGSAC Conference on Computer and Communications Security*. 2705–2718.

[84] Chrysoula Stathakopoulou, Michael Wei, Maofan Yin, Hongbo Zhang, and Dahlia Malkhi. 2023. BBCA-LEDGER: High Throughput Consensus meets Low Latency. *arXiv preprint arXiv:2306.14757* (2023).

[85] Nick Szabo. 1997. Formalizing and securing relationships on public networks. *First monday* (1997).

[86] N. Szabo. 1997. The Idea of Smart Contracts. <http://www.fon.hum.uva.nl/rob/Courses/InformationInSpeech/CDROM/Literature/LOTwinterschool2006/szabo.best.vwh.net/idea.html>

[87] Yong Chiang Tay, Nathan Goodman, and Rajan Suri. 1985. Locking performance in centralized databases. *ACM Transactions on Database Systems (TODS)* 10, 4 (1985), 415–462.

[88] Parth Thakkar and Senthilnathan Natarajan. 2020. Scaling hyperledger fabric using pipelined execution and sparse peers. *arXiv preprint arXiv:2003.05113* (2020).

[89] Parth Thakkar and Senthilnathan Natarajan. 2021. Scaling blockchains using pipelined execution and sparse peers. In *Proceedings of the ACM Symposium on Cloud Computing*. 489–502.

[90] Parth Thakkar, Senthil Nathan, and Balaji Viswanathan. 2018. Performance benchmarking and optimizing hyperledger fabric blockchain platform. In *2018 IEEE 26th international symposium on modeling, analysis, and simulation of computer and telecommunication systems (MASCOTS)*. IEEE, 264–276.

[91] Gang Wang, Zhijie Jerry Shi, Mark Nixon, and Song Han. 2019. Sok: Sharding on blockchain. In *Proceedings of the 1st ACM Conference on Advances in Financial Technologies*. 41–61.

[92] Yu Chen Wang, Angela Demke Brown, and Ashvin Goel. 2023. Integrating Non-Volatile Main Memory in a Deterministic Database. In *Proceedings of the Eighteenth European Conference on Computer Systems*. 672–686.

[93] Zhaoguo Wang, Shuai Mu, Yang Cui, Han Yi, Haibo Chen, and Jinyang Li. 2016. Scaling multicore databases via constrained parallel execution. In *Proceedings of the 2016 International Conference on Management of Data*. 1643–1658.

[94] Gavin Wood et al. 2014. Ethereum: A secure decentralised generalised transaction ledger. *Ethereum project yellow paper* 151, 2014 (2014), 1–32.

[95] Jiang Xiao, Shijie Zhang, Zhiwei Zhang, Bo Li, Xiaohai Dai, and Hai Jin. 2022. Nezha: Exploiting concurrency for transaction processing in dag-based blockchains. In *2022 IEEE 42nd International Conference on Distributed Computing Systems (ICDCS)*. IEEE, 269–279.

[96] Jie Xu, Yingying Cheng, Cong Wang, and Xiaohua Jia. 2021. Occam: A secure and adaptive scaling scheme for permissionless blockchain. In *2021 IEEE 41st International Conference on Distributed Computing Systems (ICDCS)*. IEEE, 618–628.

[97] Di Yang, Chengnian Long, Han Xu, and Shaoliang Peng. 2020. A review on scalability of blockchain. In *Proceedings of the 2020 2nd International Conference*

on Blockchain Technology. 1–6.

[98] Chang Yao, Divyakant Agrawal, Gang Chen, Qian Lin, Beng Chin Ooi, Weng-Fai Wong, and Meihui Zhang. 2016. Exploiting single-threaded model in multi-core in-memory systems. *IEEE Transactions on Knowledge and Data Engineering* 28, 10 (2016), 2635–2650.

[99] Maofan Yin, Dahlia Malkhi, Michael K. Reiter, Guy Golan Gueta, and Ittai Abraham. 2019. HotStuff BFT Consensus with Linearity and Responsiveness. In *Proceedings of the ACM Symposium on Principles of Distributed Computing*. ACM, 347–356. <https://doi.org/10.1145/3293611.3331591>

[100] Haifeng Yu, Ivica Nikolić, Ruomu Hou, and Prateek Saxena. 2020. Ohie: Blockchain scaling made simple. In *2020 IEEE Symposium on Security and Privacy (SP)*. IEEE, 90–105.

[101] Xiangyao Yu, George Bezerra, Andrew Pavlo, Srinivas Devadas, and Michael Stonebraker. 2014. Staring into the abyss: An evaluation of concurrency control with one thousand cores. (2014).

[102] Xiangyao Yu, Andrew Pavlo, Daniel Sanchez, and Srinivas Devadas. 2016. Tic-toc: Time traveling optimistic concurrency control. In *Proceedings of the 2016 International Conference on Management of Data*. 1629–1642.

[103] Yuan Yuan, Kaibo Wang, Rubao Lee, Xiaoning Ding, Jing Xing, Spyros Blanas, and Xiaodong Zhang. 2016. Bcc: Reducing false aborts in optimistic concurrency control with low cost for in-memory databases. *Proceedings of the VLDB Endowment* 9, 6 (2016), 504–515.

[104] Mahdi Zamani, Mahnush Movahedi, and Mariana Raykova. 2018. Rapidchain: Scaling blockchain via full sharding. In *Proceedings of the 2018 ACM SIGSAC conference on computer and communications security*. 931–948.

[105] Luyi Zhang, Yujue Wang, Yong Ding, Hai Liang, Changsong Yang, and Chunhai Li. 2023. Sharding Technologies in Blockchain: Basics, State of the Art, and Challenges. In *International Conference on Blockchain and Trustworthy Systems*. Springer, 242–255.

[106] Yan Zhang, Jia Kang Wang, and Ying Jie Han. 2023. CChain: a high throughput blockchain system. In *Second International Conference on Digital Society and Intelligent Systems (DSIns 2022)*, Vol. 12599. SPIE, 129–136.

[107] Hao Zhou, Ming Chen, Qian Lin, Yong Wang, Xiaobin She, Sifan Liu, Rui Gu, Beng Chin Ooi, and Junfeng Yang. 2018. Overload control for scaling wechat microservices. In *Proceedings of the ACM Symposium on Cloud Computing*. 149–161.

Processing the transactions of shard S on replica R :

```

1: Let  $txn\_list$  be a transaction list storing the transactions from clients.
2: event Receive a transaction  $T$  of shard  $S'$  from client do
3:   if  $S \neq S'$  then
4:     Redirect  $T$  to the shard submitter of  $S'$ .
5:   Return.
6:   Append  $T$  to  $txn\_list$ .

7: event Receive a batch  $B$  of transaction from  $txn\_list$  do
8:   outcomes  $O = \text{Execute}(B)$ 
9:   Deliver  $B_r = \langle B, O, r \rangle$  to  $\text{DAG}(B_r, r)$ 
10:  event Receive a Shard reconfiguration  $S'$  do
11:    Start a new DAG
12:    Start to process the transactions of shard  $S'$ .

```

Figure 17: Preplay.

```

1: event Receive a valid block  $B_r$  of shard  $S$  sent from replica  $R$  at round  $r$  from
DAG do
2:   if  $R$  is not the shard submitter of  $S$  at round  $r$  then
3:     Return invalid
4:   Build the dependency graph  $G$  based on the read/write set  $S$  in  $B_r$ .
5:   Execute the transactions simultaneously using  $G$  and verify the results.
6:   if All the results are matched with the ones included in  $B_r$  then
7:     Return valid
8:   else
9:     Return invalid

10:  event Commit blocks  $B$  from the committer at round  $r$  from consensus do
11:    for Each block  $b$  from round  $r$  of sub-DAG  $j$  in  $B$  do
12:      if  $b$  is a Shift block then
13:        num_committed_shift_block += 1
14:        Continue
15:        Update the values in the write sets to the storage.
16:      if num_committed_shift_block ==  $2f + 1$  then
17:        Reconfig the shard submitter to the next shard.
18:        num_committed_shift_block=0

```

Figure 18: Validate blocks.

Proposing a block B at round r on replica R :

```

1: event Receive  $2f + 1$  blocks  $\{B\}$  at round  $r - 1$  do
2:   need_shift = false
3:   if  $\{B\}$  contains  $f + 1$  Shift blocks then
4:     need_shift = true
5:   else
6:     for each replica  $R$  do
7:       if Do not receive any block from  $R$  after round  $r - K$  then
8:         need_shift = true
9:       if  $K'$  blocks have been proposed then
10:         need_shift = true
11:   if need_shift = true and  $R$  does not send  $B_{shift}$  in the current DAG then
12:     Generate  $B_{shift}$  and deliver to other replicas
13:   else
14:     Deliver block  $B$  to other replicas
15:   Go to the next round

```

Figure 19: Broadcast the Shift block at round r if blocks from some replicas are missing from round $r - K$ or K' blocks have been proposed to make a periodical rotation.

Appendix A Concurrent Executor Implementation

We demonstrate the implementation of each component in *CE* in this section.

A.1 Execution on the Executors

Figure 20 shows the pseudocode code of the executors in *CE*. When *CE* receives a batch B of transactions, it initiates a set of executors

```

1: Let cc be the instance of CC.
2: Let result_list be the execution outcomes for the transactions.
3: Let cid be the cid assigned by CC if the transaction is read-only.
4: Initial cid = -1.

5: function Execute (Batch b)
6:   Initial the result_list: result_list.clear()
7:   Initial a new instance CC: cc.init()

8:   for Each transaction T in Batch b do
9:     Deliver T to the executor to execute
10:    Wait for the results for all the transactions in
11:    Return result_list

12: event Receive an abort of transaction T from CC do
13:   Abort T if the executor of T is alive
14:   Deliver T to the executor to re-execute
15:   Commit T: cc.commit(T)

16: event Receive a commit notification with  $\langle T, cid, RES, V \rangle$  do
17:   result.append( $\langle T, cid, RES, V \rangle$ )

Executor :
18: event Receive a transaction T do
19:   Notify CC to clean the state of T: cc.StartTxn(T)
20:   Leverages eEVM to execute T

21: event Read key K, transaction T do
22:   Return cc.read(K, T)

23: event Write key K with value V, transaction T do
24:   Return cc.write(K, V, T)

```

Figure 20: Executor Implementation.

and runs the eEVM [58], a tool to execute smart contracts, to execute the contract code. eEVM provides the read and write callback functions for the developers to implement their implementations to read and write the values for each key. When the read and write functions are triggered, *CE* will send the operation to *CC* (Line 22 and 24). If an abort of a transaction *T* is received from *CC* due to the conflict with other transactions, the execution will be aborted and *T* will be re-sent to the executor to re-execute. When eEVM completes the execution, the executor will commit the transaction (Line 15).

As discussed in Section 7.2, the transaction is not actually committed after sending the commit request to *CC*. *CC* will send a notification after the transaction is finalized and *CE* can obtain the results (Line 17). Once all the transactions are committed, *CE* returns their scheduled orders (the commit order), read/write sets, and operation results.

A.2 Concurrency Controller

Concurrency Controller (*CC*) will receive four types of operations: Write, Read, Commit. *CC* will check if the transactions have been aborted before processing. The algorithm is shown in Figure 21 and Figure 22.

A.2.1 Write OP. When *CC* receives a write operation O_k from a transaction *T* with key *K* to update the value to *V*, If O_k is a new record, *CC* will add the necessary edges to the graph by linking all the non-write nodes (defined in Section 8.1) to ensure the graph is valid as depicted in Section 8.2. If adding the record failed due to a cycle detected, abort *T* by removing the node or processing cascading abort (Line 1 in Figure 22).

```

1: Let G be the dependency graph.
2: Let commit_list be the list saving the transactions waiting for commit.

3: function StartTxn (transaction T)
4:   Clean the abort state of T if it is aborted.

5: function Write (key K, value Vnew, transaction T)
6:   if T has been aborted then
7:     Return Fail
8:   Let u be the node of transaction T.
9:   if u is a new node on K then
10:    if G.AddNewWriteRecord(u, Vnew, K) returns Fail then
11:      AbortNode(u)
12:      Return Fail
13:    Return Success

14: function Read (key K, transaction T)
15:   if T has been aborted then
16:     Return Fail
17:   Let u be the node of transaction T.
18:   if u is a new node on K then
19:     u = G.AddNewReadRecord(u, K)
20:   else
21:     u' = u
22:   if u' does not exist then
23:     AbortNode(u)
24:     Return Fail
25:   V is the lastest updating value key K on u'.
26:   Add a new record  $\langle R, K, V \rangle$  to u
27:   Return V

28: function Commit (transaction T)
29:   if T has been aborted then
30:     Return Fail
31:   Let u be the node of transaction T.
32:   if u contains dependency edges in G then
33:     commit_list.append(T)
34:   else
35:     CommitNode(u)
36:     Remove T from commit_list
37:     for each transaction T' in commit_list do
38:       Let u' be the node of transaction T.
39:       if u' does not have dependency in G then
40:         Commit(T)

```

Figure 21: CC implementation of processing transactions.

A.2.2 Read OP. Similar to the write OP, if the read operation O_k from *T* is a new record, *CC* returns the value and adds the necessary edges to the graph by linking all the write nodes. While adding the record, the graph will return the node *u*' the record refers to (Line 19 in Figure 21) which is the node *T* reads *K* from. If *u*' does not exist due to conflicts detected, abort *T*.

A.2.3 Commit. When receiving a commit request to inform the execution is done for transaction *T*, *CC* will place *T* to a pending list (*commit_list*) if there is any dependency for *T* in the graph (Line 33 in Figure 21). Otherwise, commit the nodes and generate the read/write sets *RWS* and the values of all the reads *V*. The commit order *cid* which is the scheduled order for the transactions is obtained. Then *CC* will notify the executors that transaction *T* has been committed, with the outcomes $\langle T, cid, RWS, V \rangle$.

Upon a transaction *T* has been committed, it will check if there is any other transaction waiting in *commit_list* that it is allowed to commit as its dependency has been removed (Lines 37-40).

A.3 Dependency Graph

Figure 23 shows how the Dependency Graph is constructed in *CC*. When adding a write record to node *u* on key *K*, the graph will

```

1: function AbortNode (node  $u$ , transaction  $T$ )
2:   if  $u$  is not a write node on every key then
3:     Remove( $u$ )
4:   else
5:     CasadingAbort( $u$ )
6:   Mark  $T$  is aborted.
7:   Send notification to the executors.

8: function CommitNode (node  $u$ , transaction  $T$ )
9:    $RWS$  is the read/write sets
10:   $V$  is all the read results
11:  for Each record  $< Type, Key, Value >$  in  $u$  do
12:     $RES$ .append( $< Type, Key >$ )
13:    if  $Type = R$  then
14:       $V$ .append( $< Key, Value >$ )
15:     $cid$  = Commit( $T$ )
16:  Notify  $CE$  with  $< T, cid, RES, V >$ 

```

Figure 22: CC implementation of committing and aborting transactions.

ensure all the non-write nodes on key K , which only reads the value on K , have the paths to u (Line 7). After adding the edges, a cycle check will be triggered to detect the conflict (Line 12).

On the other hand, when adding a read record on node u , u tries to obtain the value from an incoming node x (Line 30). If no such node, a write node of key K will be searched or using the root node instead. When adding the edges from node x , some other edges will be added to ensure the graph is valid (Lines 23-25). Finally, returning the referring node x to CC .

Appendix B Thunderbolt Security Analysis

In this section, we first provide the evidence of the correctness of CE . Then we proof the safety and liveness of Thunderbolt.

B.1 Correctness of CE

Suppose CE generates a sequential order $SO = [T_1, \dots, T_n]$ and produces an outcome $OUT = [OUT_1, \dots, OUT_n]$ for a set of transactions. Let SE be the sequential execution in SO . Let the outcomes OUT' be the outcomes of SE .

B.1.1 Causal Ordering. Before giving proofs, we define notions for the causal ordering. The causal ordering of transactions in distributed systems is introduced by Lamport by defining a well-known "happened before" relation, denoted \rightarrow [54]. If A and B are two events, then $A \rightarrow B$ if and only if one of the following conditions is true:

- (1) A occurs before B in the same location;
- (2) A is an outgoing message, and B corresponds to the response message;
- (3) There is an existing event C that $A \rightarrow C$ and $C \rightarrow B$;

We extend the causal ordering from events to transactions in concurrency control to define a causal relationship between two transactions A and B :

Definition 1. If transaction A needs to be executed before B , $A \rightarrow B$, if and only if B reads the data updated by A .

Definition 2. A and B can be executed concurrently only if $A \not\rightarrow B$ and $B \not\rightarrow A$.

Definition 3. If A has a causal relationship with B , either $A \rightarrow B$ or $B \rightarrow A$.

```

1: Let  $root$  is the root node.

2: function AddNewWriteRecord (node  $u$ , value  $V$ , key  $K$ )
3:    $link\_to\_root = true$ 
4:   for each non-write node  $v$  containing records on  $K$  do
5:     if  $v$  does not contain any outgoing edge on  $K$  then
6:       /* No other nodes depending on  $v$  on  $K$  */
7:       Add edges( $v, u, K$ )
8:        $link\_to\_root = false$ 
9:     if  $link\_to\_root == true$  then
10:      Add edges( $root, u, K$ ) /* Link to root */
11:    else
12:      if Contain a cycle on  $u$  then
13:        Return Fail
14:      Return Success

15: /* Find a write node  $x$  on  $K$  and depend on  $x$  then return the value from  $x */$ 
```

```

16: function AddNewReadRecord (node  $u$ , key  $K$ )
17:   /* Find a incoming node  $x$  on key  $K$  */
18:    $x = GetIncomingNode(u, K)$ 
19:   if  $x! = None$  then
20:      $x = GetWriteNodeToRead(u, K)$ 
21:   if  $x! = None$  then
22:     Add edges( $x, u, K$ ) /* Link to  $x$  */
23:     for Each write node on  $w$  key  $K$  do
24:       if No path from  $w$  to  $x$  on  $K$  then
25:         Add edges( $w, x, K$ )
26:       Return  $x$ 
27:     Add edges( $root, u, K$ ) /* Link to root */
28:     Return  $root$ 

29: /* Find a incoming node  $x$  on key  $K$  */
30: function GetIncomingNode (node  $u$ , key  $K$ )
31:   if  $u$  contains any incoming read node  $v$  of  $u$  on key  $K$  then
32:     if CheckCycle( $v, u, K$ ) == Fail then
33:       Return  $v$ 
34:     if  $u$  contains any incoming write node  $v$  of  $u$  on key  $K$  then
35:       if CheckCycle( $v, u, K$ ) == Fail then
36:         Return  $v$ 
37:       Return None

38: /* Find a write node  $x$  to read on key  $K$  */
39: function GetWriteNodeToRead (node  $u$ , key  $K$ )
40:   for each write node  $v$  containing records on  $K$  do
41:     if CheckCycle( $v, u, K$ ) == Fail then
42:       Return  $v$ 
43:     Return None

44: /* Check if a read node  $v$  can read values on node  $u$  on key  $K$  */
45: function CheckCycle (node  $u$ , node  $v$ , key  $K$ )
46:   if  $u$  is not a write node on key  $K$  then
47:     /* read values from a node without any update will not affect the graph */
48:     Return Fail
49:   for Each write node on  $w$  key  $K$  do
50:     /* need to ensure  $u$  is the last update */
51:     if Contain a path from  $v$  to  $w$  then
52:       /* a cycle occurs  $u \rightarrow v \rightarrow w \rightarrow u$  */
53:       Return Fail
54:   Return Success

```

Figure 23: Dpendency Graph Implementation.

Definition 4. If $A \rightarrow B$ and $B \rightarrow C$, then $A \rightarrow C$.

B.1.2 Proof of Serializability. If CE is serializable, $OUT = OUT'$.

Definition 5 (Read-Complete). If T_i reads a value from T_j in the execution in Thunderbolt, T_i will also read the value from T_j in SE .

Definition 6 (Write-Complete). If T_i and T_j both write new values on K but T_i commits before T_j in the execution in Thunderbolt, T_i will also write the values on K before T_j when in SE .

THEOREM 7. CE is both Read-Complete and Write-Complete if the dependency graph G is always valid.

PROOF. Firstly, if G is valid, we know that if there is a read node R_v^k reading a value from a write node W_u^k on key K , all the write nodes writing values on K either have a path to u or have a path from v to guarantee the correctness of read after write. Therefore, if transaction T_i reads values on T_j on key K , all other transactions writing values will not be assigned an order between T_i and T_j . Thus, T_i will read the same value on T_j , and CE is Read-Complete.

Secondly, since SO is the commit order in CE , if T_i commits before T_j , T_i will be assigned before T_j in SO . Thus, T_j will update the values after T_i in SE and CE is Write-Complete. \square

THEOREM 8. CE is serializable iff CE is both Read-Complete and Write-Complete.

PROOF. For any transaction T_i in SO , if T_i reads some values on transactions $T_j \leq T_i$ in CE , T_i must read the same values in SE since CE is Read-Complete. If T_i writes some new values since CE is Write-Complete, T_i will write the same values in SE , and all the transactions $T_j < T_i$ have been committed. Thus, the transactions will produce the same outcomes in CE and SE : $OUT = OUT'$. \square

B.2 Safety of Thunderbolt

Thunderbolt produces the sequential order SO and the read/write sets for each transaction. If the read/write set RS_i of transaction T_i overlaps the read/write set RS_j of transaction T_j and $T_i \rightarrow T_j$ in SO , T_j has a dependency on T_i . Therefore, if T_i depends on T_j in one validator, the other validators will have the same dependency. Finally,

all the validators contain the same dependency graph generated by the read/write sets and SO . Thus, following the dependency graph to execute the transactions leads them to obtain the same outcomes.

B.3 Liveness of Thunderbolt

If all the replicas behave well, they will keep proposing the blocks in the same DAG. All the blocks proposed by each shard submitter will be committed eventually. When a malicious replica is detected, honest replicas will propose a Shift block. If less than $2f + 1$ Shift blocks are proposed, the DAG will not be switched and all the replicas will stay in the current DAG and keep proposing the new blocks. If there are $2f + 1$ Shift blocks, all the honest replicas will switch to the new DAG in the same round (section 2.2). After at least $2f + 1$ honest replicas have relocated to the new DAG, they are able to propose the new blocks.

If all the replicas behave properly, they will consistently propose blocks within the same DAG. Each shard submitter will eventually have the blocks they proposed committed. Upon detecting a malicious replica, honest replicas will propose a Shift block. If fewer than $2f + 1$ Shift blocks are proposed, the DAG will remain unchanged, and all replicas will persist within the current DAG, continuing to propose new blocks. If there are $2f + 1$ Shift blocks, all honest replicas will transition to the new DAG in the same round (section 2.2). Following the relocation of at least $2f + 1$ honest replicas to the new DAG, they will have the capability to propose new blocks.